ITERATIVE MULTIUSER DETECTION FOR ULTRA-WIDEBAND SYSTEMS

WANG XIAOLI

NATIONAL UNIVERSITY OF SINGAPORE

2004

ITERATIVE MULTIUSER DETECTION FOR ULTRA-WIDEBAND SYSTEMS

WANG XIAOLI

(B.Eng. University of Electronic Science & Technology of China)

A THESIS SUBMITTED

FOR THE DEGREE OF MASTER OF ENGINEERING

DEPARTMENT OF ELECTRICAL & COMPUTER ENGINEERING

NATIONAL UNIVERSITY OF SINGAPORE

2004

Acknowledgements

I would like to express my sincere appreciate to my supervisors, Prof. Ko Chi Chung and Dr. Huang Lei, for their invaluable guidance, advice, encouragement, and patience throughout my research work and this thesis.

Special thanks to my parents and my boyfriend, who always love and care for me. It's their encouragement and support made me pull through all the difficulties.

I also want to thanks all the students and staffs from Communications Lab in Department of Electrical & Computer Engineering. Their friendship made my life colorful and meaningful.

Last but not least, I'm grateful for National University of Singapore for giving me the opportunity to pursue my postgraduate study.

Contents

List of Figures

List of Tables

Abbreviations

2G	second-generation
3G	third-generation
ARake	all-Rake
AWGN	additive white Gaussian noise
BER	bit error rate
BPAM	binary phase amplitude modulation
BPPM	binary pulse position modulation
CDMA	code division multiple access
CM	channel model
DS	direct-sequence
FCC	Federal Communications Commission
GSM	global system for mobile communications
IFI	inter-frame interference
IR	impulse radio
ISI	inter-symbol interference
LMS	least mean square
LOS	line of sight
MAC	medium access control
MAI	multiple access interference
MAP	maximum *a posteriori*
MF	matched filter
ML	maximum-likelihood
MMSE	minimum mean squared error
MOE	minimum output energy
MRC	maximum ratio combining
MSE	mean squared error

MUD	multiuser detection
NLOS	none line of sight
OFDM	orthogonal frequency division multiplexing
OOK	on-off keying
PAM	pulse amplitude modulation
PDP	power density profile
PHY	physical layer
PPM	pulse position modulation
PRake	partial Rake
RF	radio frequency
RLS	recursive least square
SER	symbol error rate
SIC	soft interference canceller
SIR	signal-to-interference ratio
SISO	soft-input soft-output
SNR	signal-to-noise ratio
SRake	selective Rake
SS	spread-spectrum
ST	space-time
TH	time-hopping
UWB	ultra-wideband
WLAN	wireless local area network
WMAN	wireless metropolitan area network
WPAN	wireless personal area networks
WWAN	wireless wide area network

Summary

Ultra-Wideband (UWB) technology has drawn considerable attention among both researchers and practitioners over the past few years. It offers a solution for the bandwidth, cost, power consumption and physical size issues in wireless personal area networks (WPAN), and enables wireless connectivity with consistent high data rate across multiple devices.

Research on multiuser detection (MUD) for achieving high data rate, low complexity, and good performance for multiple access UWB systems has already been carried out. Among which iterative MUD methods seem especially interesting for their ingenious design. In this thesis a low-complexity iterative MUD algorithm for UWB systems is proposed, together with the extension of this algorithm to Space-Time (ST) coded multi-antenna UWB systems, where the complexity is further reduced.

The proposed iterative MUD algorithm is specifically designed for UWB systems. In addition, a chip-based discrete-time signal model is constructed to achieve noticeable simplicity. During the detection process, the maximum *a posteriori* (MAP) criterion is applied by subtracting the multiple access interference (MAI) precisely. Considering the asynchronous scenario, which means the transmitted symbols from different users (transmitters) are not synchronized, a truncated detection window is introduced, and the computational

complexity for this block decoding is reduced in an iterative manner. The key features of this proposed algorithm is its low complexity and good BER performance, which approaches to that of the single-user system.

Aiming to combine the advantages of both UWB technology and ST coding, we have extended this algorithm to ST coded multi-antenna UWB systems. After using an analog ST coding scheme, we also find a way to counteract the problem caused by asynchronous transmission, and the structure of a detection window lasting several symbols is simplified into a two-symbol by two-symbol detection model.

Chapter 1

Ultra-Wideband Overview

Ultra-Wideband (UWB) technology, a rising and promising technology in wireless personal area networks (WPAN), has attracted much attention lately in both academia and industry. This chapter begins with an introduction to UWB technology, followed by a technical overview of UWB signal and channel modeling. Finally the outline of this thesis is given.

1.1 Introduction to UWB

Over the past 100 years, great advances have been achieved in wireless communication technologies. Personal communication devices now enable communications everywhere on the planet.

Wireless communication networks can be classified into different types based on the distances over which data can be transmitted [1].

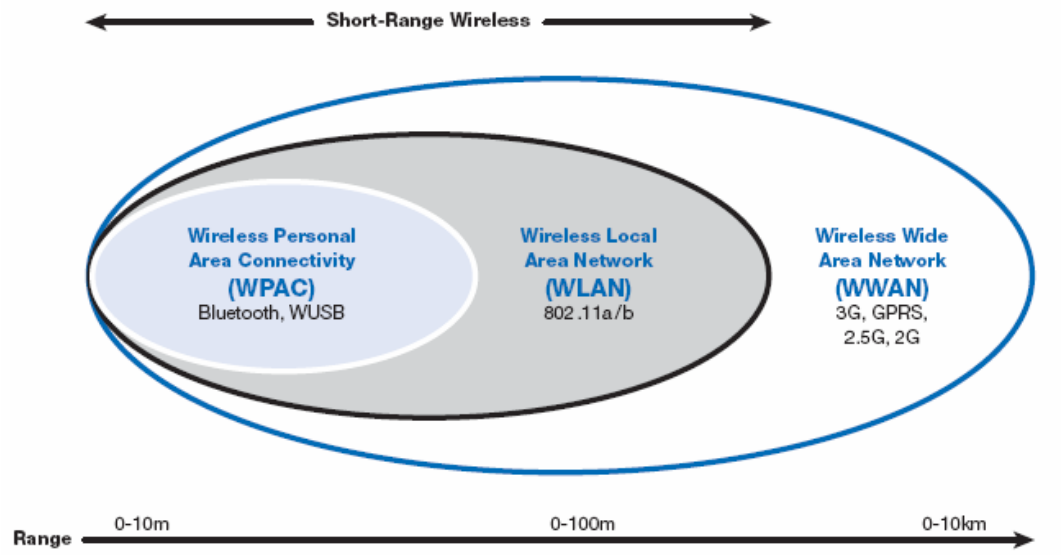

Fig. 1.1. Coverage range of wireless communication networks.

Firstly, the wireless wide area network (WWAN), with a transmission radius of tens of kilometers. Current WWAN technologies are known as the second-generation (2G) system, including key technologies like Global System for Mobile communications (GSM) or Code Division Multiple Access (CDMA), and the third-generation (3G) technologies that would follow a global standard and provide world wide roaming capabilities.

Secondly, the wireless metropolitan area network (WMAN), with a transmission radius of several kilometers. It enables users to establish wireless connections between multiple locations within a metropolitan area without the high cost of laying fiber or copper cabling and leasing lines. Different technologies such as the multi-channel multi-point distribution service and the local multipoint distribution services are being used. The IEEE 802.16 working group for broadband wireless access standards is still developing specifications to standardize development of these technologies.

The third type is the wireless local area network (WLAN), with a transmission radius on the order of hundreds of meters. It can operate in two different ways, either the infrastructure WLAN or the peer-to-peer (ad-hoc) WLAN. In 1997, IEEE approved the 802.11 standard for WLAN, which specifies a data transfer rate of 1 to 2 megabit per second (Mbps). Under 802.11b, which is commonly known as “Wi-Fi”, data is transferred at a maximum rate of 11 Mbps over a frequency band on the 2.4 gigahertz (GHz) [3].

The last one is the wireless personal area network (WPAN) or wireless personal area connectivity (WPAC), with a transmission range on the order of tens of meters or even less. WPAN technologies enable users to establish ad-hoc, wireless communications for devices that are used within a personal operating space. Currently, the two main WPAN technologies applied now are Bluetooth and infrared light. IEEE has established the 802.15 working group for WPAN. Goals for these standards are low complexity, low power consumption, interoperability and the coexistence with 802.11 networks.

In WPAN today, wireless connectivity has enabled a new mobile lifestyle filled with conveniences for mobile computing users. While consumers may soon demand more convenient and high-speed connections among their PCs, personal digital recorders, MP3 players, digital camcorders and cameras, high-definition TVs, set-top boxes, game systems, personal digital assistants, and cell phones in the office or home [2]. Fortunately, UWB technology offers a solution for the bandwidth, cost, power consumption and physical size requirements of the next-generation consumer requirements. And UWB enables wireless connectivity

with consistent high data rate video and audio streams across multiple devices and PCs throughout the office or home.

1.2 UWB Technology

1.2.1 Technology Considerations

UWB technology is loosely defined as any radio or wireless transmission schemes that occupy a bandwidth greater than 20 percent of the center frequency, or a bandwidth of at least 500 MHz. It was first used in radar systems and has recently generated much interest in short-range wireless communications, which is in part resulted from the U.S. Federal Communications Commission's (FCC) action, specifying a usable spectrum bandwidth between 3.1 GHz and 10.6 GHz for UWB radio [2].

UWB differs substantially from conventional narrowband radio frequency (RF) and spread spectrum (SS) technologies. It transmits very short pulses typically on the order of a fraction of a nanosecond, thereby spreads the energy from near D.C. to a few gigahertz. As can be seen from Fig. 1.2, Bluetooth, 802.11a/g, cordless phones, and numerous other devices are relegated to the unlicensed frequency bands that are provided at 900 MHz, 2.4 GHz, and 5.1 GHz. Each radio channel is constrained to occupy only a narrow band of frequencies, relative to what is allowed for UWB [4].

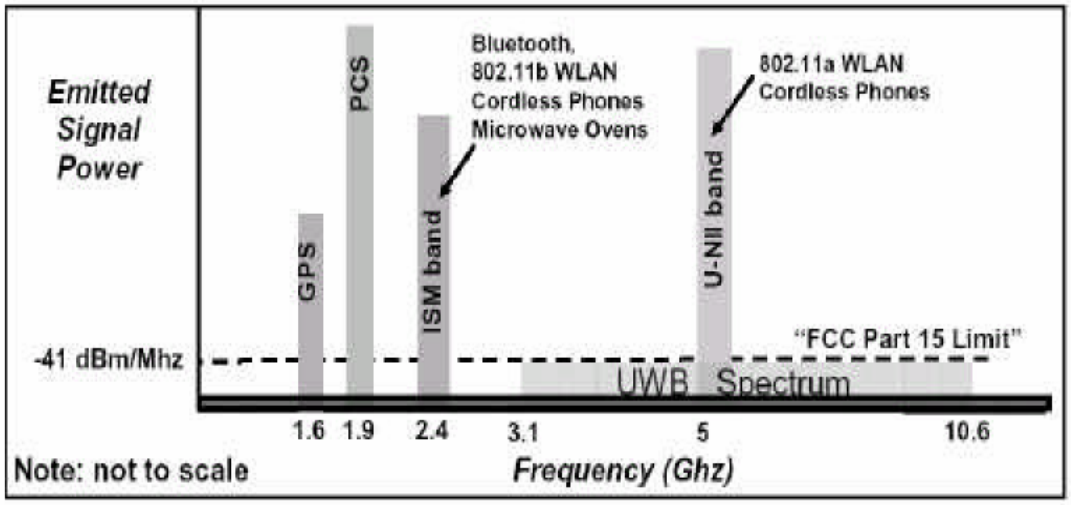

Fig. 1.2 UWB spectrum allocation .

Based on Shannon's Capacity Limit Equation, which states that the maximum channel capacity grows linearly with the channel bandwidth while grows logarithmically with the signal to noise ratio, a greatly improved channel capacity can be achieved by UWB due to its ultra-wide bandwidth. As shown in Fig. 1.3, other standards now under development of the Bluetooth Special Interest Group and IEEE 802 working groups would boost the peak speeds and spatial capacities of their respective systems still further, but none appear capable of reaching that of UWB [4].

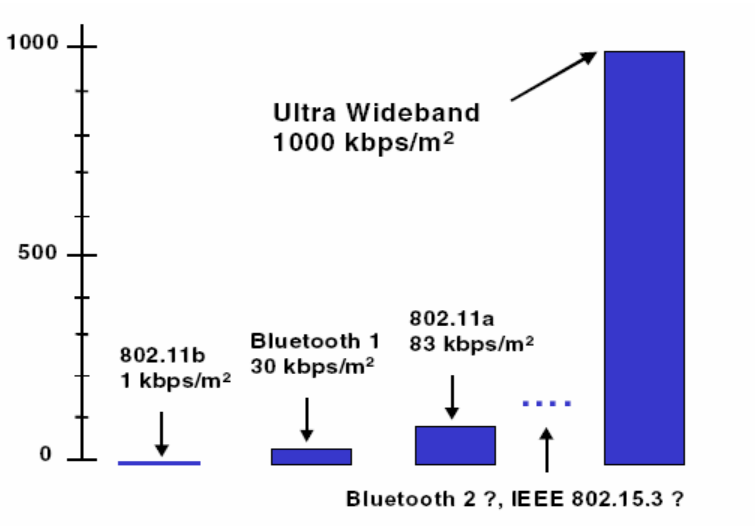

Fig. 1.3. Spatial capacity comparisons of 802.11, Bluetooth, and UWB.

UWB technology also allows spectrum reuse. A cluster of devices can communicate on the same channel as another cluster of devices in another room without causing interference due to such a short range that UWB-based WPAN has. An 802.11g WPAN solution, however, would quickly use up the available bandwidth in a single device cluster, which would be unavailable for reuse anywhere else in the office or home.

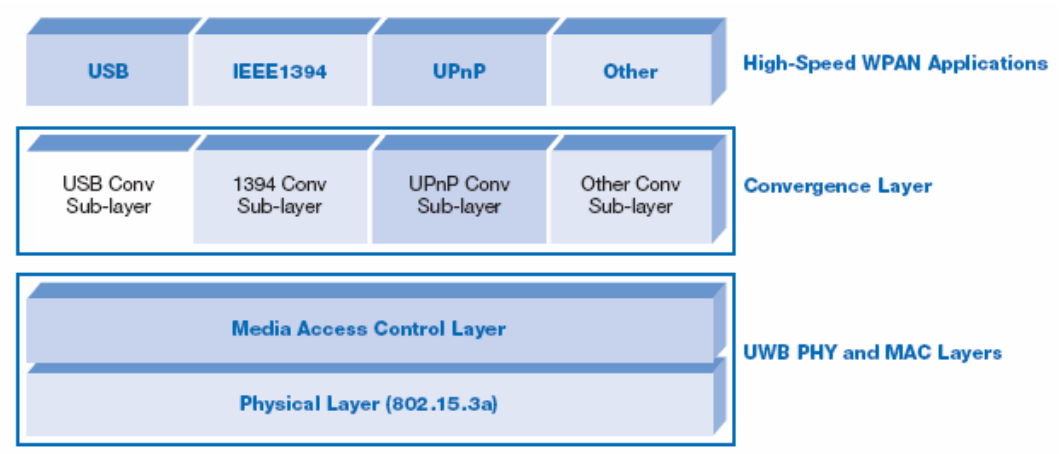

Fig. 1.4. Application and protocol layers for UWB.

Fig. 1.4, taken from [2], reveals the full solution stack required to make UWB a viable radio alternative in the marketplace.

1.2.2 Advantages and Disadvantages

The uniqueness of UWB technology would offer many advantages over normal narrowband systems. However, the main challenge for UWB system also comes from its ultra-wide bandwidth. Table 1.1, partly taken from [5], gives a summary of the advantages, disadvantages, and applications of UWB properties.

Table 1.1. Advantages, disadvantages, and applications of UWB properties.

UWB Properties	Advantages	Disadvantages	Applications
Very wide fractional and absolute RF bandwidth	● High rate communications ● Potential for processing gains ● Low frequencies penetrate walls and grounds	● Potential interference to existing systems ● Potential interference from existing systems	● High-rate WPAN ● Low-power and stealthy communications ● Multiple access
Very short pulses	● Direct resolvability of discrete multipath components ● Diversity gain	● Large number of multipaths ● long synchronization times	● Low-power combined communications and localization
Persistence of multipath reflections	● Low fade margins ● Low power	● Scatter in angle of arrival	● None line of sight (NLOS) communications indoors
Carrierless transmission	● Hardware simplicity ● Small hardware	● Inapplicability of super-resolution beamforming	● Smart sensor networks

1.3 UWB Signal Model

UWB systems can be divided into two groups: single-band and multi-band. Two commonly used single-band impulse radio systems are time-hopping spread-spectrum impulse radio (TH-UWB) and direct-sequence spread-spectrum impulse radio (DS-UWB). In TH-UWB, a pseudorandom sequence defines the time when the pulses are transmitted, and in DS-UWB, the pulses are transmitted continuously using a pseudorandom sequence for the spreading of information bits. Multi-band UWB divides the spectrum between 3.1 to 10.6 GHz into several bands that are at least 500 MHz wide. In each band, multi-band UWB system transmits one pulse and waits until the echoes have died off, which gives low inter-frame interference (IFI) but high data rates since all bands are occupied in parallel [6].

Throughout this thesis we would restrict our discussion to single-band TH-UWB systems.

1.3.1 Monocycle

UWB signals can be modeled by impulse-shaped functions called Monocycles. The two types of monocycles generally in use are the Gaussian monocycle and the Scholtz's monocycle. The latter is named so because it first appeared in Scholtz's paper [7]. Here we will look into details of the second one.

The Scholtz's monocycle is similar to the second derivative of the Gaussian pulse, which can be represented as

$$\omega(t) = A\left[1 - 4\pi\left(\left(t - T_c/2\right)/\tau_m\right)^2\right]\exp\left[-2\pi\left(\left(t - T_c/2\right)/\tau_m\right)^2\right]. \quad (1.1)$$

Fig. 1.5 is the waveform and spectrum of the Scholtz's monocycle, where A is the normalized amplitude, T_c is the chip width, and τ_m is half of the pulse width.

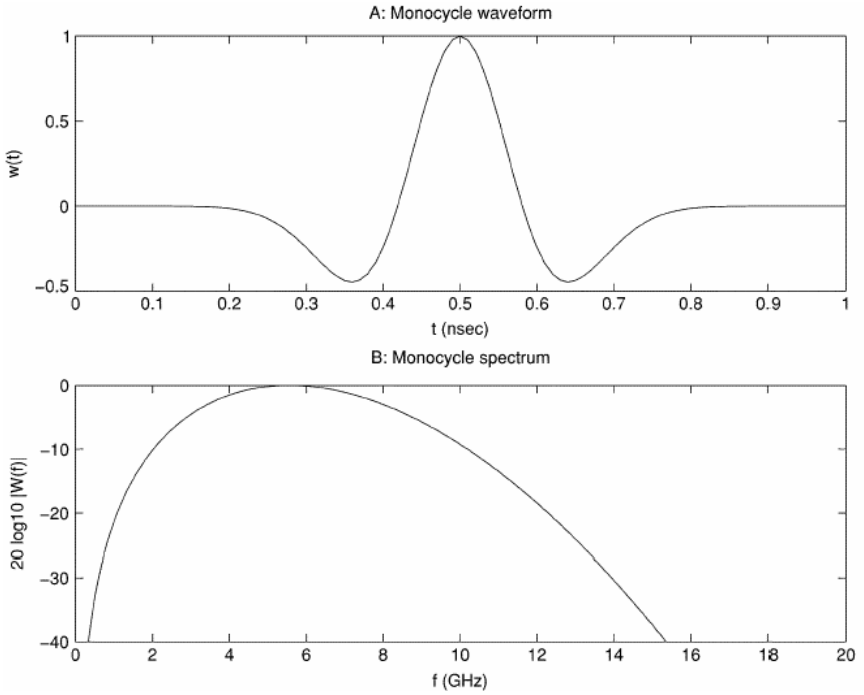

Fig. 1.5. The Scholtz's monocycle waveform and spectrum.

1.3.2 Time-Hopping

The typical TH format employed by UWB can be found in [9]:

$$s^{(k)}(t) = \sum_{p=0}^{\infty}\sum_{j=0}^{N_f-1}\omega(t - pT_s - jT_f - c_j^{(k)}T_c), \quad (1.2)$$

where $s^{(k)}(t)$ is the signal transmitted from the k^{th} transmitter, which is made up of a pulse train. Hence, N_f is the number of monocycles used for representing a single symbol, also known as the number of frames within a symbol, T_f is the frame duration, and T_s is the symbol duration. Another concept here is the "chip",

a smaller unit under "frame", also the smallest addressable time delay bin. Besides, T_c stands for the chip duration and N_c stands for the number of possible chips within a frame, i.e., $T_f = N_c T_c$. To minimize collisions among multiple users, each user is assigned a distinctive TH sequence $c_j^{(k)} \in [0, N_c]$, where j=1, …, N_f, and $c_j^{(k)} T_c$ determines the additional time-shift added to the j^{th} monocycle of each symbol from transmitter k.

1.3.3 Modulation

The data modulation of UWB signals can be chosen from Pulse Position Modulation (PPM), Pulse Amplitude Modulation (PAM), as well as On-Off Keying (OOK). After a certain kind of modulation, the transmitted signal of the TH-UWB system can be written as [9]:

$$s^{(k)}(t) = \sum_{p=0}^{\infty} \sum_{j=0}^{N_f - 1} A h_p^{(k)} \beta_j^{(k)} \omega(t - pT_s - jT_f - c_j^{(k)} T_c - \delta \alpha_j^{(k)}). \tag{1.3}$$

With $\beta_j^{(k)}$ changing the amplitudes of the pulses (OOK, PAM) or $\delta \alpha_j^{(k)}$ varing the positions of the pulses (PPM), UWB signals can be modulated in different ways as shown in Table 1.2.

Table 1.2. UWB Modulation Options

Binary Schemes	$\beta_j^{(k)}$	$\delta\alpha_j^{(k)}$
BPPM	1	0, T_c
BPAM	a_1, a_2	0
OOK	0, a	0
M-ary Schemes	$\beta_j^{(k)}$	$\delta\alpha_j^{(k)}$
M-ary PPM	1	mT_c (m = 0, 1, …, M-1)
M-ary PAM	$2m$-1-M (m = 1, 2…, M)	0

1.4 UWB Channel Modeling

UWB technology is applicable to short-range wireless communications under severe multipath fadings. The investigation of UWB channel models has long been popular and quite a lot have been presented, basically based on field tests and measurements.

Here we would introduce Intel's UWB channel model, which was proposed by Jeff Foerster in Feb. 2003 in [10], and has been approved by the study group IEEE 802.15.SG3a. According to different realizations, Four types of channel models (CM) have been specified, i.e., CM1, 0~4 meters' range with line of sight (LOS); CM2, 0~4 meters' range with none line of sight (NLOS); CM3, 4~10 meters' range, NLOS; and CM4, greater than 10 meters' range, NLOS.

Fig. 1.6 to Fig. 1.9 are typical channel responses for CM1 to CM4.

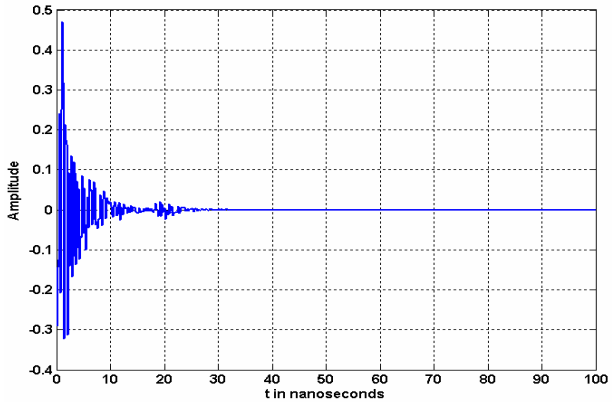

Fig. 1.6. Typical channel response of CM1.

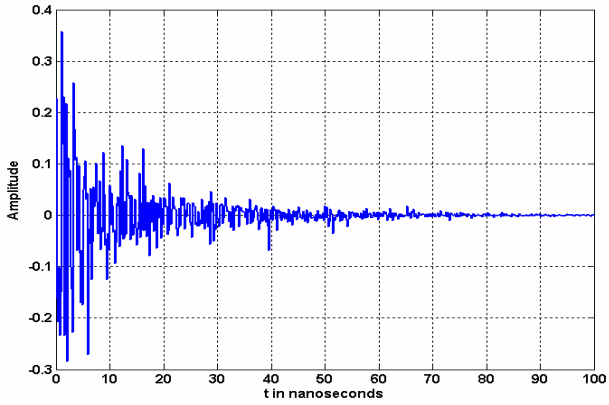

Fig. 1.7. Typical channel response of CM2.

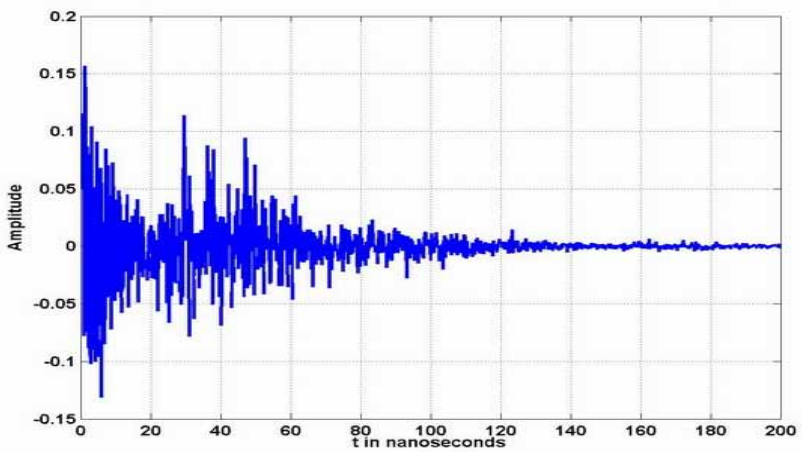

Fig. 1.8. Typical channel response of CM3.

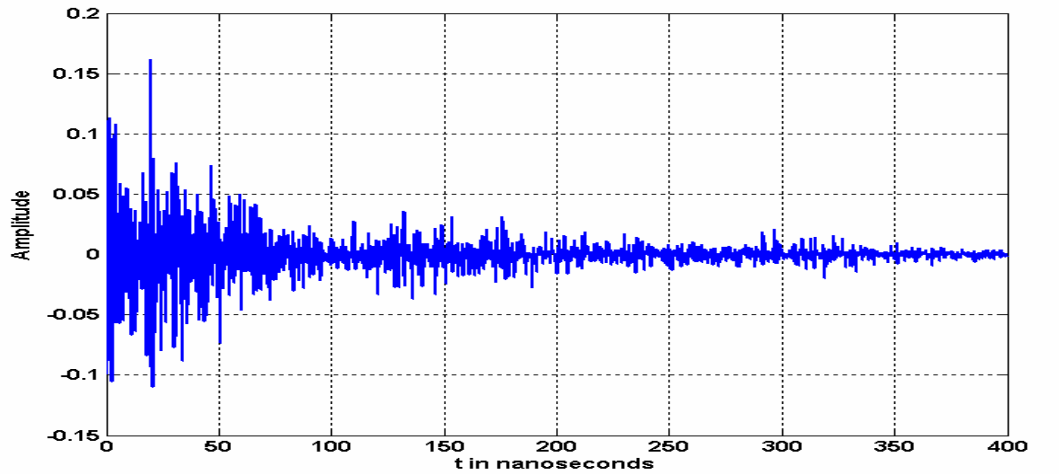

Fig. 1.9. Typical channel response of CM4.

1.5 Organization of the Thesis

Accurate and effective multiuser detection (MUD) algorithms are quite important and attractive issues for multiple-access UWB communication systems. Among which, iterative MUD seems especially interesting for its ingenious design and low-complexity. In this thesis, we mainly consider the MUD issues in TH-UWB systems, and focus on a proposal of a low-complexity iterative MUD algorithm as well as its even lower-complexity extension to ST coded multi-antenna UWB systems.

In Chapter 2, several popular multiuser receivers for UWB systems are addressed, namely the advanced Rake receivers, the optimum multiuser receiver, the adaptive MMSE (minimum mean squared error) multiuser receiver, and the iterative interference cancellation multiuser receiver.

A novel low-complexity iterative MUD algorithm specifically designed for UWB systems is proposed in Chapter 3. The maximum *a posteriori* (MAP)

criterion is applied in the detection process and the MAI is subtracted in an iterative manner. Considering the asynchronous scenario, a truncated detection window is introduced, which leads to a kind of block decoding. Simulation results are also provided to verify the theoretical analysis of the proposed algorithm.

The low-complexity extension of the iterative MUD algorithm to ST coded multi-antenna UWB systems is provided in Chapter 4, which aims to combine the advantages of both UWB technology and ST coding. By using an analog ST coding scheme, a way to counteract the problem caused by asynchronous transmission is found, and further simplification is achieved. Simulation results demonstrate its satisfactory BER performance and low complexity.

Finally, Chapter 5 concludes the thesis and recommends possibilities for future work.

Chapter 2

Multiuser Detection for UWB Systems

Along with the increasing interest in UWB communications, motivation for pertinent MUD is induced for multiple access UWB systems. Typical existing MUD algorithms for UWB communications will be described in this chapter.

2.1 Advanced Rake Receivers

Actually a large number of Rake-related receivers may not be classified as multiuser receivers. The elements behind these Rake-related receivers is to model the MAI as a Gaussian random variable by assuming strict power control and a large number of users. While in practical systems neither perfect power control nor large enough number of users can be assumed to justify the use of the Gaussian approximation.

However, Rake related receivers still hold a favorable place in MUD issues

within UWB systems. They are often implemented as a part in the MUD process, or act in the performance comparisons. This is why we would like to begin our introduction with them.

2.1.1 ARake, SRake and PRake

A standard and "ideal" Rake receiver that combines all the resolvable multipath components is called All-Rake (ARake). However, the complexity of the receiver structure (a great number of correlators required) seems not worth the performance it achieves. Thus complexity-reduced Rake receivers are proposed by researchers, which are based on either selective combining (SRake) or partial combining (PRake) [11].

Assume that there is altogether L_a available resolve multipath components for a certain UWB channel corresponding to a specific pair of transmitter and receiver. The SRake selects the L_b best paths (under the least severe fading) from all the available ones and combines this subset with the maximum ratio combining (MRC). Notice that in order to make a proper selection it has to keep track of all multipath components.

A much lower complexity can be achieved in PRake. The PRake uses the first L_p arriving paths out of the L_a, which are not necessarily the best. The complexity reduction with respect to the SRake is due to the absence of the selection mechanism, where only the position of the first arriving path is needed.

Fig.2.1, taken from [11], plots the bit error probability (BEP) of these three kinds of "Rake" receivers vs. the average signal-to-noise ratio (SNR) at the

receiver output, and with a reference distance d = 1m. The solid and dashed lines represent the UWB channels having the same average power-delay profile (PDP), and under respectively "Nakagami" and "Rayleigh" fading (referring to [11] for details).

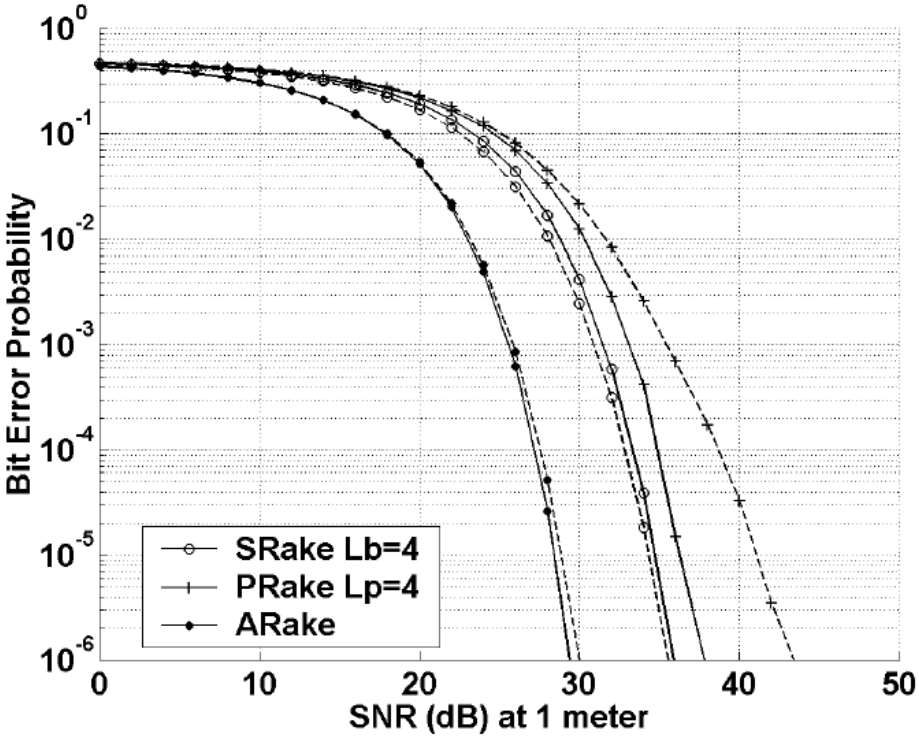

Fig. 2.1. The BEP for the ARake, SRake and PRake (taken from [11]).

2.1.2 Rake MMSE

Instead of the normal MRC, other methods are also usable, like the recently proposed Rake MMSE combining for UWB systems [12] [13]. It can be considered as either an enhancement of the normal Rake reception, or a reduced complexity alternative of the adaptive MMSE MUD.

Here we present a comparison between the Rake MRC and Rake MMSE. Fig.

2.2, taken from [13], compares the structure of the specified receivers. The classical Rake receiver shown in Fig. 2.2 a) is with *n* arms, and combined via MRC using side information on the received amplitude for each Rake arm. The Rake MMSE receiver shown in Fig. 2.2 b) is also with *n* arms, while the adaptive filter would perform MMSE-combining of the Rake arms.

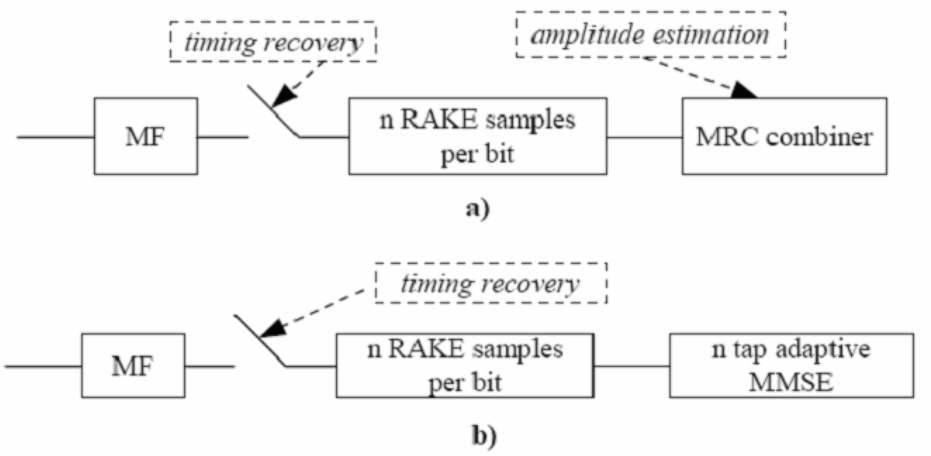

Fig. 2.2. Receiver structure comparison: a) Rake MRC; b) Rake MMSE .

Fig. 2.3, presented in [13], compares the bit error rate (BER) performance of *n*-arm Rake MRC, *n*-arm Rake MMSE and MUD MMSE. The simulation is carried out under NLOS UWB channels in the presence of 5 UWB interferers, where all with the same received power. As for Fig. 2.4, shown in [13] also, one narrow-band interferer is added in (an IEEE 802.11a OFDM signal), with the received signal-to-interference ratio (SIR) equals to -30 dB.

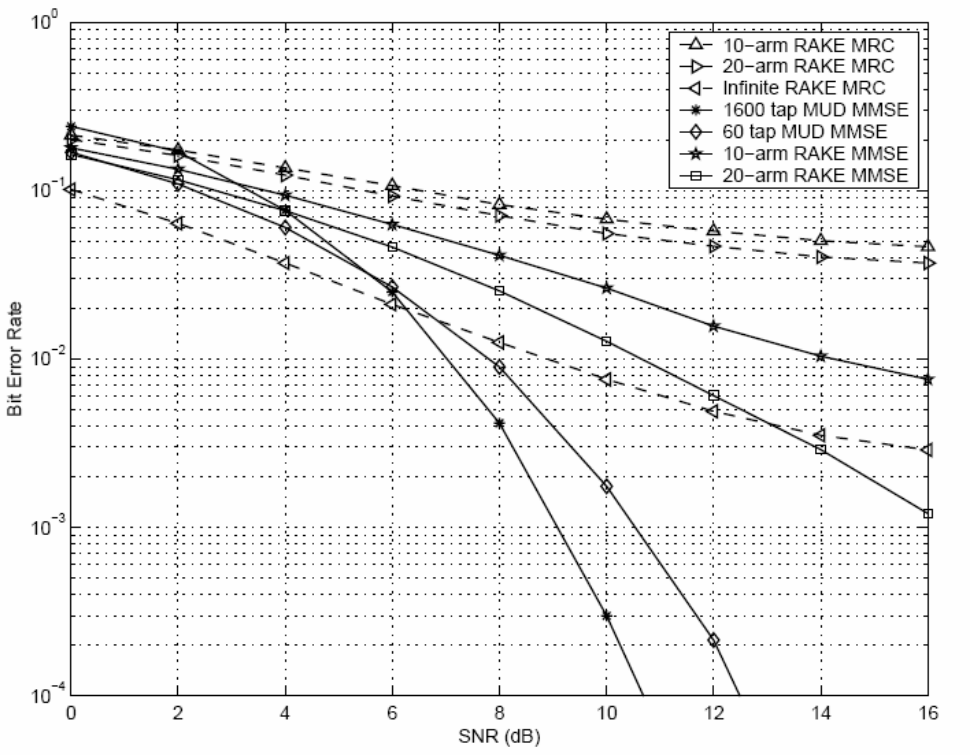

Fig. 2.3. BER performance comparison (taken from [13]).

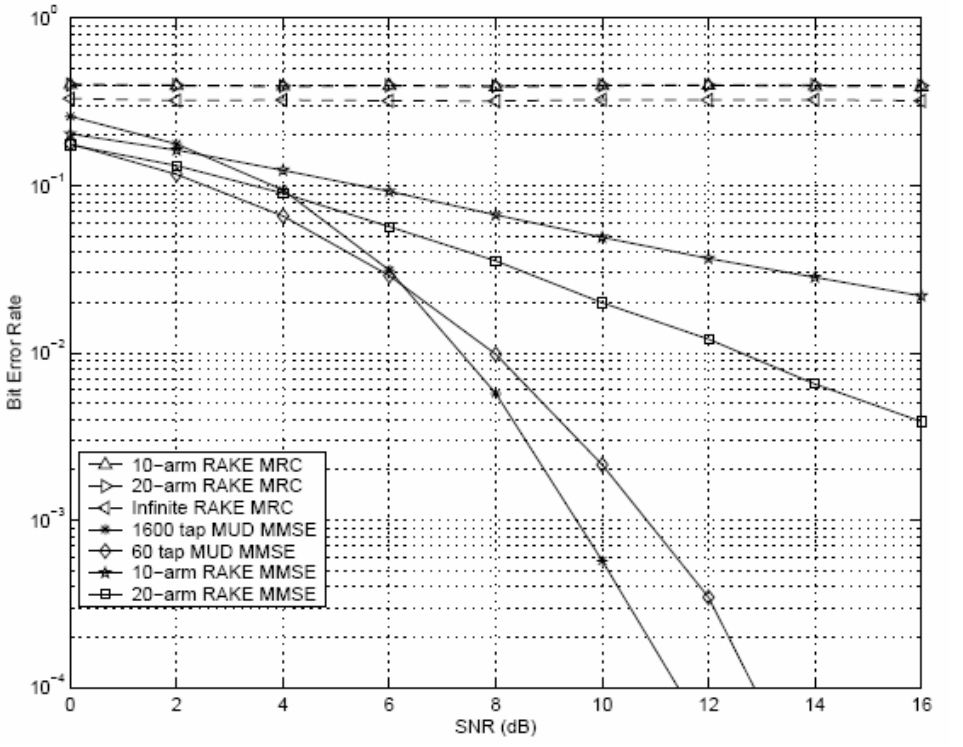

Fig. 2.4. BER performance comparison with SIR=-30 dB (taken from [13]).

Seen from the simulation results, the differences among these three kinds of MUD are obvious. The Rake MRC has little resistance to the MAI; the Rake MMSE performs better but not very well; and the MUD MMSE achieves a quite satisfactory BER performance.

2.2 Optimum Multiuser Detection

It is well known that optimum multiuser detectors are double-edged for both good BER performance and high complexity. Though optimum MUD may not be easily applied in practice, theoretically it still acts as the benchmark for other methods. The following is an introduction to the optimum MUD in UWB systems, and the detailed derivations can be found in [14].

Upon feeding the received signal into a bank of correlator receivers, a compact representation can be constructed as in (2.1), where y is the correlator output vector, R is the correlation matrix, A is the signal energy matrix, b is the symbol vector, and η is the noise vector at the receiver output.

$$y = RAb + \eta . \tag{2.1}$$

The optimum MU detector makes use of the statistics generated by the correlator bank across all N_u active users and performs joint maximum-likelihood (ML) sequence detection. It selects the sequence b which maximizes the likelihood function, which also means minimizes $||y - RAb||^2$, across $M^{N_u N_s}$ possible realizations of b. Here M is the M-ary orthogonal signaling and N_s is the

length of symbols under consideration. Its decision rule is thus:

$$\hat{b} = \arg \min_{b} \left\| y - RAb \right\|^2 . \tag{2.2}$$

The search for the optimum b is a combinatorial optimization problem detailed in [15, Chapter 4], where its complexity grows exponentially with N_u.

Fig. 2.5 is a simulation result presented in [14], the symbol error rate (SER) comparison for the conventional 2-PPM single-user detector and the optimum MU detector in a UWB system with two active users. The relative user delays are 0 and T_c, respectively, and the bit energy $E_b = E_s / \log_2 M$. It is assumed $T_s > N_u M T_c$ such that the optimum MU detector reduces to the optimum joint ML symbol detector for $N_s = 1$ [14]. Referring to this figure, the optimum MUD achieves a performance near to that of the single-user detector.

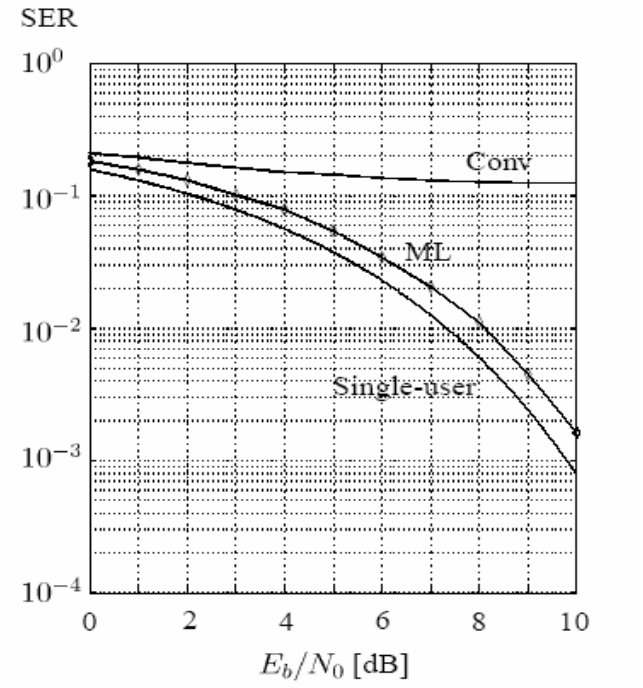

Fig. 2.5. SER comparison: optimum MUD vs. single-user detection (taken from [14]).

2.3 Adaptive MMSE Multiuser Detection

In [16], DS-CDMA UWB receivers are developed to combine the power of both UWB and DS-CDMA techniques. The authors demonstrate that the adaptive MMSE MUD receiver is able to gather multipath energy and reject inter-symbol and inter-chip interference to a much greater extent than RAKE receivers with 4 or 8 arms, and they also show that the adaptive MMSE is able to reject a narrowband IEEE 802.11a OFDM interferer.

The MMSE receiver consists of a bandpass filter and an adaptive filter. The bandpass filter suppresses noise and interference that outside of the signal bandwidth to increase the SNR. The adaptive filter is a FIR (finite impulse response) filter that essentially acts as a correlator. At each bit epoch, a bit decision is made at the correlator output and is then fed back to the adaptive filter. The observation window of the filter is typically longer than 1 bit interval and, therefore, windows overlap in time. Tap weights for the adaptive filter are adjusted adaptively using least mean square (LMS) or recursive least squares (RLS) algorithms.

Fig. 2.6, presented in [16], is the BER performance in NLOS UWB channels in the presence of 15 UWB interferers, where all with the same received power. We see that all RAKE receivers are overcome by the MAI, and even the infinite RAKE exhibits flat BER of about 10%. The analytical results for the MMSE show about a 4-dB penalty relative to the AWGN (additive white Gaussian noise) case while increasing the system throughput dramatically. The high sampling rate RLS

algorithm is able to capitalize on the MAI rejection capability, achieving the analytical bounds in high SNR region. The low sampling rate RLS performs considerably worse, but shows no error floor.

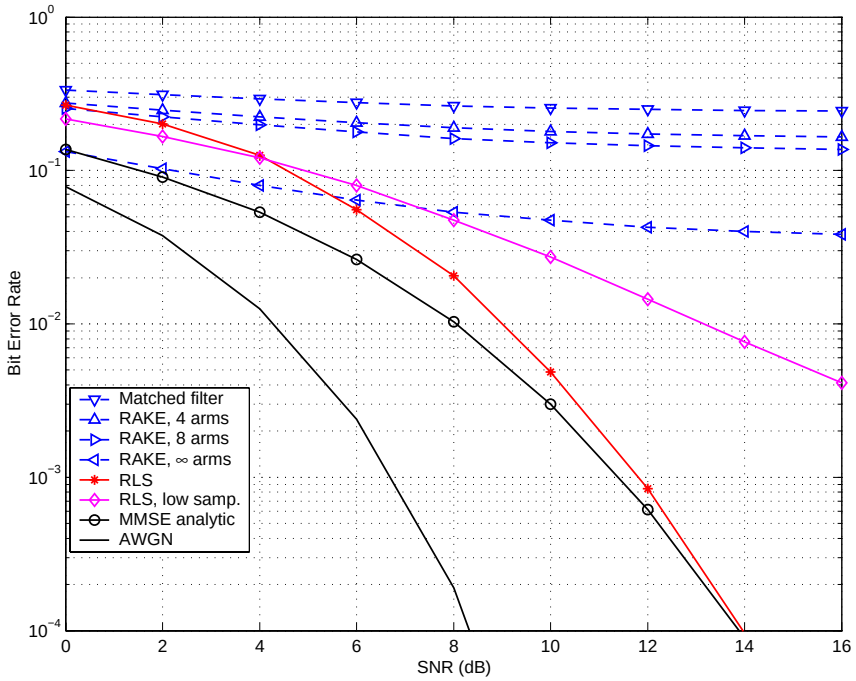

Fig. 2.6. BER in the presence of 15 interfering users (taken from [16]).

Fig. 2.7, also presented in [16], is related to the same situation but with one OFDM interferer, where the SIR = (Power of UWB / Power of OFDM) = 0 dB. The LMS and RLS algorithms are now able to reject the narrow band interference and are only limited by the MAI, while the RAKE receivers have the same flat performance as in Fig. 2.6.

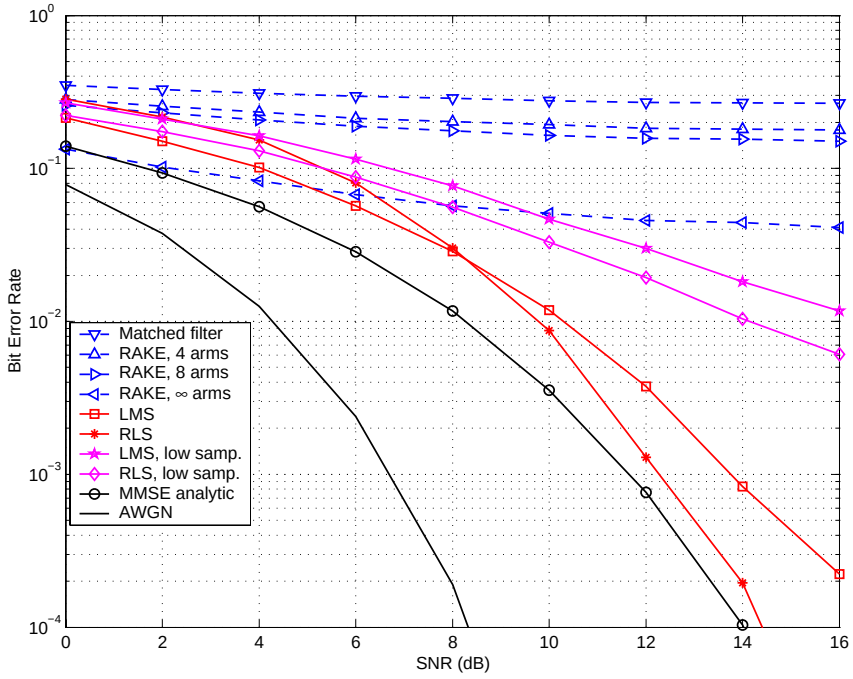

Fig. 2.7. BER in the presence of 15 users and one interferer (taken from [16]).

2.4 Iterative Interference Cancellation & Decoding

In the following, we would like to introduce an iterative interference cancellation and decoding algorithm for UWB systems in multipath channels using MMSE filters [17].

The block diagram of the iterative interference cancellation receiver structure is shown in Fig. 2.8. It consists of a bank of soft interference cancellers (SIC), followed by a block of MMSE filters. The outputs of these filters are then fed to a bank of likelihood calculators (LC), each followed by a soft-input soft-output (SISO) convolutional decoder, from where the information is fed back to SICs for the purpose of interference cancellation.

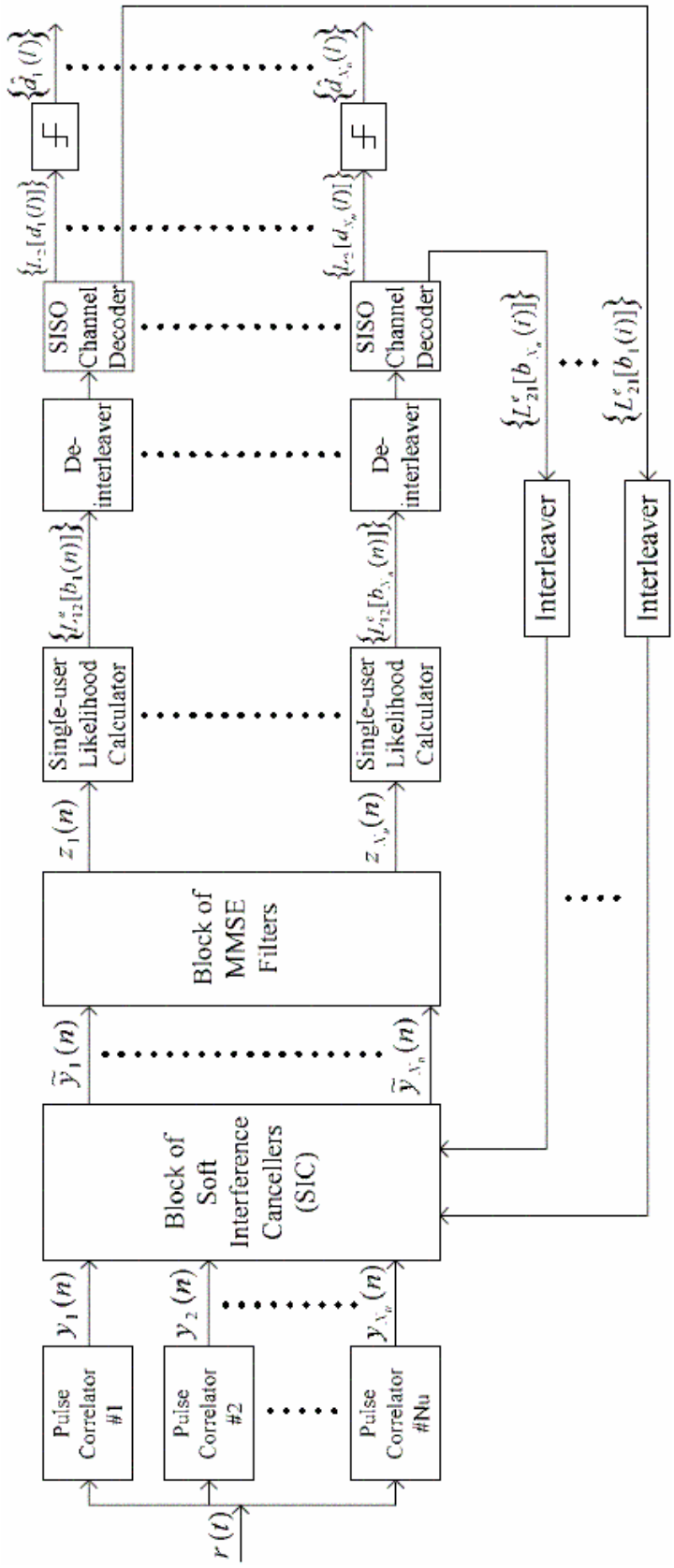

Fig. 2.8. Block diagram of the iterative interference cancellation receiver.

Fig. 2.9 and Fig. 2.10, shown in [17], illustrate the BER vs. received SNR of this iterative interference cancellation and decoding method, where the numbers of active users are 3 and 4, respectively. The plots of BER for a single-user coded system and a multiuser uncoded system are also given. As can be realized for the coded system, the proposed iterative receiver performs about 1-2 dB better than the non-iterative MMSE receiver at BER of about 10^{-2}.

A main disadvantage of the proposed receiver is that it is only applicable to synchronous systems, that is, the transmitted symbols from different users (transmitters) are synchronized, and this seems to be an unrealistic assumption. In addition, its structure and computational complexities are quite high.

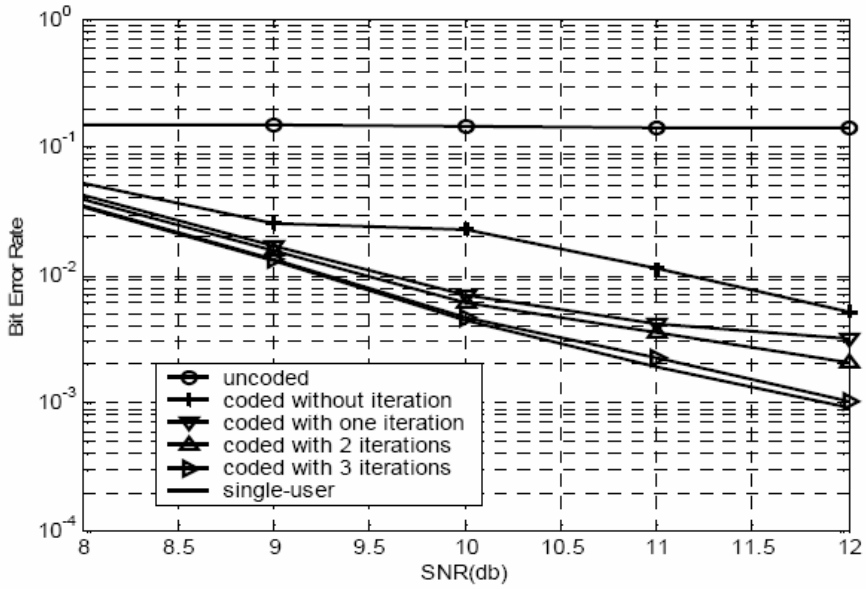

Fig. 2.9. BER versus SNR with 3 active users (taken from [17]).

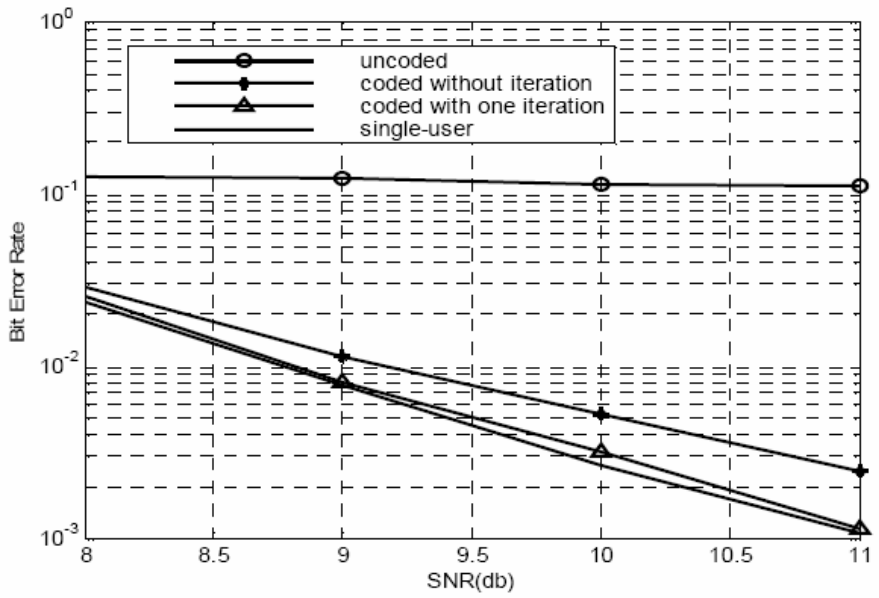

Fig. 2.10. BER versus SNR with 4 active users (taken from [17]).

2.5 Summary

Several popular multiuser receivers are introduced in this chapter, namely the advanced Rake receivers, the optimum multiuser receiver, the adaptive MMSE multiuser receiver, and the iterative interference cancellation receiver. It should be noted that most of the existing MUD schemes for UWB are somewhat simple applications of standard MUD methods to UWB systems, and may not be quite satisfactory in terms of both the complexity and the performance. For UWB systems, advanced multiuser detectors should be specifically designed.

Chapter 3

Iterative Multiuser Detection for UWB Systems

Accurate and effective MUD algorithms are quite important and attractive issues for multiple-access UWB communication systems. Among which, iterative MUD seems especially interesting for its ingenious design and low-complexity [18]-[21]. Inspired by the recently proposed iterative MUD for synchronous TH-IR systems [22]-[23], we present in this chapter a low-complexity iterative MUD algorithm for asynchronous UWB systems.

3.1 System Model

Consider a binary-PAM TH-UWB system with N_u active users. Let $b(k,p)$ be the information (1 or -1) corresponding to the k^{th} user's p^{th} symbol. Based on general UWB signal models, the transmitted signal of the k^{th} user can be given as:

$$s_k(t) = \sum_{p=0}^{\infty} \left[b(k,p) \sum_{j=0}^{N_f - 1} \omega\left(t - pT_s - jT_f - c_k(j)T_c\right) \right], \tag{3.1}$$

where T_s, T_f and T_c are defined as symbol duration, frame duration and chip duration respectively, N_f and N_c are the number of frames within a symbol and number of chips within a frame respectively, $c_k(j) \in [0, N_c)$ represents the pseudorandom TH code related to the k^{th} user's j^{th} frame, thus $c_k(j)T_c$ is the additional time shift of the k^{th} user's j^{th} pulse for the purpose of avoiding collisions among different users. And $\omega(t)$ is the typical UWB pulse shape, which is purposely chosen so that the pulse duration is equal to the chip duration T_c.

Multipath fading channels are under consideration, which are assumed to be known and quasi-static over the duration of one symbol. The received signal $y(t)$ is thus the sum of the signals across all the active users in addition to white Gaussian noise:

$$y(t) = \sum_{k=1}^{N_u} \sum_{p=0}^{\infty} \left\{ b(k,p) \sum_{l=1}^{N_p} \left[\gamma_{k,p}(l) \sum_{j=0}^{N_f - 1} \omega\left(t - pT_s - jT_f - \left(c_k(j) + l\right)T_c - \tau_k\right) \right] \right\} + \xi(t), \tag{3.2}$$

where τ_k is the relative delay of the k^{th} user from the 1^{st} one. Without loss of generality we set τ_1=0 and $0 \le \tau_k < T_s$. And $\xi(t)$ is an AWGN with a spectral density of $N_0/2$ (also with a variance of σ_0^2). $\gamma_{k,p}(l)$ is the gain of the l^{th} multipath related to the k^{th} user's p^{th} symbol, with a corresponding delay of lT_c after the instance of transmission. Note that the definition of multipath here is based on consecutive chip width labeled 1 to L backwards. For normal indoor environment in which UWB systems work, most of the energy carried by

multipaths is limited in the duration of one frame, thus we let L (the maximum number of multipaths under consideration) around N_c, and ignore the others (if there is any).

As will be explained later, the chip width T_c is set as the least resolvable time slot in the system model, thus τ_k is assumed to be multiples of T_c. This chip-based integration of channel information may give rise to consecutive resolvable multipaths, which may lead to noticeable convenience for our chip-based signal model, and thus our detection algorithm.

As shown in Fig. 3.1, the received signal $y(t)$ is passed through a bank of N_u matched filters (MF), and each aims to capture the strongest path of the coming pulses of the specified user. Since the channel information is known, after a comparison of the amplitude of several first-arrival-paths (normally within 5), we can get the information about the strongest path. Let $l_{k,p}T_c$ represents the delay of the strongest path of the pulses corresponding to the k^{th} user's p^{th} symbol, then the sampling instances can be easily figured out as:

$$\sum_{p=0}^{\infty}\sum_{j=0}^{N_f-1}\delta\left(t-pT_s-jT_f-\left(c_k(j)+l_{k,p}\right)T_c-\tau_k\right). \tag{3.3}$$

Notice that the $l_{k,p}$ here is different from the l appears in equation (3.2), which is a general expression of the consecutively labeled multipaths.

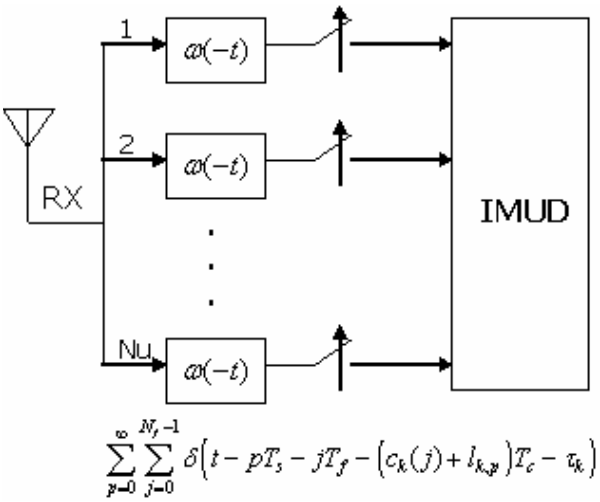

Fig. 3.1. The general receiver structure.

In order to figure out the MAI more precisely, a truncated detection window is implemented instead of the symbol-by-symbol detection. This iterative MUD algorithm is a kind of joint detection based on the maximum *a posteriori* (MAP) criterion over all complete symbols in the detection window across all active users.

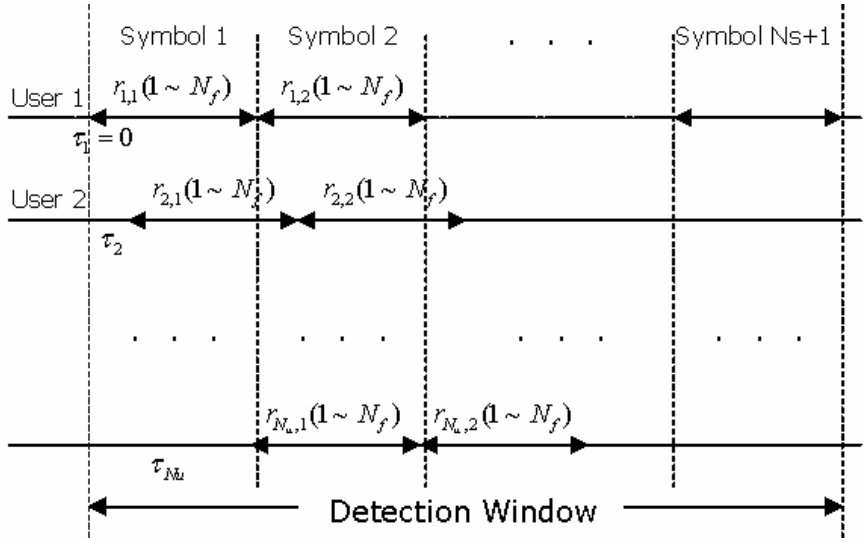

Fig. 3.2. The received sequence model in the detection window.

As shown in Fig. 3.2, $r_{k,p}(j)$ denotes the output chip-sampled value of the MF related to the k^{th} user and of the p^{th} symbol's j^{th} frame. It can be represented in (3.4) in terms of the desired pulse itself and the MAI from all the other users, where three neighboring consecutive symbols from every other user are considered in face of overlapping and multipath effects. The denotation ε_ω stands for the energy carried by the UWB pulse.

$$r_{k,p}(j)=\sum_{k'=1}^{N_u}\sum_{p'=p-1}^{p+1}\left[b(k',p')\sum_{j'=0}^{N_f-1}\gamma_{k',p'}\left(\tau_{k'}/T_c+c_{k'}(j')-\tau_k/T_c-\left(c_k(j)+l_{k,p}\right)\right)\right]\varepsilon_\omega+\eta_{k,p}(j) \tag{3.4}$$

The noise component $\eta_{k,p}(j)$ here is just the MF-output of $\xi(t)$, so it can be also assumed as a While Gaussian noise, with the variance as follows:

$$\sigma_{\eta_{k,p}}{}^2=\gamma_{k,p}^2\left(l_{k,p}\right)\sigma_0{}^2. \tag{3.5}$$

The unique point in our signal processing is to construct a discrete-time signal model for the detection and decoding process, that is, to make all the available information integrated and chip-based. In UWB communications we are dealing with super-narrow pulses on the scale of nanosecond while with relatively super-wide interspaces between the pulses. It is thus possible for us to focus on every coming pulse only and replace the continuous signal waveform with discrete-time sequence for noticeable simplicity. To be more practical, let the chip (pulse) duration T_c be the least resolvable time slot in our system model. Thus, we would have the chip-duration based multipath and MAI, the chip-sampled received signal, and also the chip-based discrete-time sequences used throughout our detection process.

3.2 Iterative Multiuser Detection

This iterative MUD algorithm is based on all the $r_{k,p}(j)$'s we've already got in the last section. Here N_u asynchronous users are addressed, and every symbol of each user is possibly interfered by at least two neighboring symbols of every other user. Thus we use a truncated detection window, with a length of (N_s+1) symbols. And after each block decoding N_uN_s detected symbols will come out together.

Let $\Phi_{k,p}$ represents the natural logarithm of the likelihood ratio of the MAP probabilities for $b(k,p)$ equaling to either 1 or -1, where k and p represent the k^{th} user and the p^{th} symbol, respectively. In the detection process, initial values of $\Phi_{k,p}$'s (k =1, …, N_u; p =1, …, N_s) are firstly set, based on which a block of new $\Phi_{k,p}$'s can be deduced with the help of channel information, and these new $\Phi_{k,p}$'s are fed back again as the initial values in the next iteration.

The following shows how to deduce $\Phi_{k,p}(n+1)$ from $\Phi_{k,p}(n)$, where n indexes the cycle of iterations.

Define:

$$\Phi_{k,p}(n+1) = \ln \frac{\Pr\left(b(k,p)=1 \mid r_{k,p}(1),\ r_{k,p}(2),\ ...,\ r_{k,p}(N_f)\right)}{\Pr\left(b(k,p)=-1 \mid r_{k,p}(1),\ r_{k,p}(2),\ ...,\ r_{k,p}(N_f)\right)}. \tag{3.6}$$

Since the $r_{k,p}$'s in the equation above are the output of the MF regarding to independent pulses, they can then be treated as independent random variables. Thus,

$$\Phi_{k,p}(n+1)=\sum_{j=0}^{N_f-1}\ln\frac{\Pr\left(b(k,p)=1\,|\,r_{k,p}(j+1)\right)}{\Pr\left(b(k,p)=-1\,|\,r_{k,p}(j+1)\right)}. \tag{3.7}$$

Based on the Bayes' rule we can further obtain:

$$\Phi_{k,p}(n+1)=\sum_{j=0}^{N_f-1}\ln\frac{\Pr\left(b(k,p)=1\right)f\left(r_{k,p}(j+1)\,|\,b(k,p)=1\right)}{\Pr\left(b(k,p)=-1\right)f\left(r_{k,p}(j+1)\,|\,b(k,p)=-1\right)}, \tag{3.8}$$

where $f(\cdot)$ represents the conditioned probability density function.

Substituting (3.4) into (3.8) we can achieve:

$$\Phi_{k,p}(n+1)=N_f\ln\frac{\Pr\left(b(k,p)=1\right)}{\Pr\left(b(k,p)=-1\right)}+ \sum_{j=0}^{N_f-1}\ln\frac{f\left(\gamma_{k,p}\left(l_{k,p}\right)\varepsilon_\omega+\sum_{k'=1}^{N_u}\sum_{p'=p-1}^{p+1}\left[b(k',p')\sum_{j'=0,*}^{N_f-1}h(k',p',j';k,p,j)\right]\varepsilon_\omega+\eta_{k,p}(j)\right)}{f\left(-\gamma_{k,p}\left(l_{k,p}\right)\varepsilon_\omega+\sum_{k'=1}^{N_u}\sum_{p'=p-1}^{p+1}\left[b(k',p')\sum_{j'=0,*}^{N_f-1}h(k',p',j';k,p,j)\right]\varepsilon_\omega+\eta_{k,p}(j)\right)}, \tag{3.9}$$

where * indicates that $k'=k$, $p'=p$, and $j'=j$ do not hold at the same time. And $h(k',p',j';k,p,j)$, explained in (3.10), stands for the channel impact suffered by the strongest path of the pulse corresponding to the k^{th} user's p^{th} symbol's j^{th} frame, caused by the pulse corresponding to the k'^{th} user's p'^{th} symbol's j'^{th} frame. Thus by multiplying the symbol information $b(k',p')$ with $h(k',p',j';k,p,j)$ and summing all them up we can calculate out the exact MAI.

$$h(k',p',j';k,p,j) =\gamma_{k',p'}\left(\left(\tau_k+pT_s+jT_f\right)\Big/T_c+c(k,j)+l_{\max}(k,p)-\left(\tau_{k'}+p'T_s+j'T_f\right)\Big/T_c-c(k',j')\right) \tag{3.10}$$

On the other hand, $\Phi_{k,p}(n)$, for any k taken from 1 to N_u and p taken from 1 to N_b, is already known during the last iteration, from its definition we can derive:

$$\begin{aligned}\Pr\left(b(k,p)=1\right) &= \Pr\left(b(k,p)=1 \mid r_{k,p}(1), r_{k,p}(2), ..., r_{k,p}(N_f)\right) \\ &= \frac{e^{\Phi_{k,p}(n)}}{1+e^{\Phi_{k,p}(n)}}\end{aligned}, \tag{3.11}$$

and

$$\begin{aligned}\Pr\left(b(k,p)=-1\right) &= \Pr\left(b(k,p)=-1 \mid r_{k,p}(1), r_{k,p}(2), ..., r_{k,p}(N_f)\right) \\ &= \frac{1}{1+e^{\Phi_{k,p}(n)}}\end{aligned}. \tag{3.12}$$

Thus we can further get:

$$\ln\frac{\Pr\left(b(k,p)=1\right)}{\Pr\left(b(k,p)=-1\right)} = \Phi_{k,p}(n), \tag{3.13}$$

and

$$\begin{aligned}E\left\{b(k,p)\right\} &= \Pr\left(b(k,p)=1\right) - \Pr\left(b(k,p)=-1\right) \\ &= \frac{e^{\Phi_{k,p}(n)}-1}{1+e^{\Phi_{k,p}(n)}} = \tanh\left(\tfrac{1}{2}\Phi_{k,p}(n)\right)\end{aligned}. \tag{3.14}$$

As we take a vast number of pulse collisions into consideration (large enough N_u), based on the Central Limit Theorem, it can be well assumed that the part of MAI in equation (3.8) has a Gaussian distribution, with *Mean*:

$$\mu_{I_{k,p}}(n) = \sum_{k'=1}^{N_u}\sum_{p'=p-1}^{p+1}\left[\tanh\left(\tfrac{1}{2}\Phi_{k',p'}(n)\right)\sum_{j'=0,*}^{N_f-1}h(k',p',j';k,p,j)\right]\varepsilon_\omega, \tag{3.15}$$

and *Variance*:

$$\sigma^2_{I_{k,p}} = \sum_{k'=1}^{N_u}\sum_{p'=p-1}^{p+1}\left[\left(1-\tanh^2\left(\tfrac{1}{2}\Phi_{k',p'}(n)\right)\right)\sum_{j'=0,*}^{N_f-1}h^2(k',p',j';k,p,j)\right]{\varepsilon_\omega}^2. \tag{3.16}$$

In accordance with (3.5) and (3.13)-(3.16), (3.9) can be further deduced as:

$$\Phi_{k,p}(n+1) = N_f \Phi_{k,p}(n) + \sum_{j=1}^{N_f} \frac{2\gamma_{k,p}\left(l_{k,p}\right)\varepsilon_{\omega}\left(r_{k,p}(j) - \mu_{I_{k,p}}(n)\right)}{\sigma^2_{I_{k,p}} + \sigma_{\eta_{k,p}}{}^2}. \tag{3.17}$$

As this iteration goes on, more and more precise values of $\Phi_{k,p}$'s can be expected. Based on simulation results, we can achieve fairly satisfactory results after only three iterations, and then make the decisions of $b(k, p)$'s according to the final signs of $\Phi_{k,p}$'s.

From the final equations (3.14), (3.15) and (3.17), it can be easily figured out that each iteration requires a computational complexity of $O(N_u^2)$, where $O(\cdot)$ represents the computational complexity function. This is much lower than that of the optimum MUD for similar system, which grows exponentially with N_u.

3.3 Simulation Results and Discussion

The computer based simulation has been carried out to validate the performance of the proposed iterative MUD algorithm for UWB systems. The channels are generated according to J. Foerster's Channel Model one [14], which is corresponding to a 0~4 meters' indoor environment with LOS components. Some prior filtrations of the available channels are made to ensure that pulses coming through the strongest path contain at least a quarter of the transmitted energy. Since channel fading is already advised in the detection process, we don't need to assume perfect power control.

In our simulation, we consider a BPAM UWB system with chip (pulse) duration T_c=1ns, number of chips within a frame N_c =50, and number of frames within a symbol N_f=10, thus each user transmits at a data rate of 2 Mbps. And based on the pulse-sampled scheme the sampling rate for all the MF is $1/T_c$ =1GHz.

Fig.3.3 shows the average mean squared error (MSE) of the detected information symbol versus the number of iterations, where both 10 and 30 active users with a 3-symbol detection window are considered. Note that the proposed iterative MUD algorithm converges promptly after around three iterations. This result also indicates that we can't expect much BER decrease by just increasing the number of iterations.

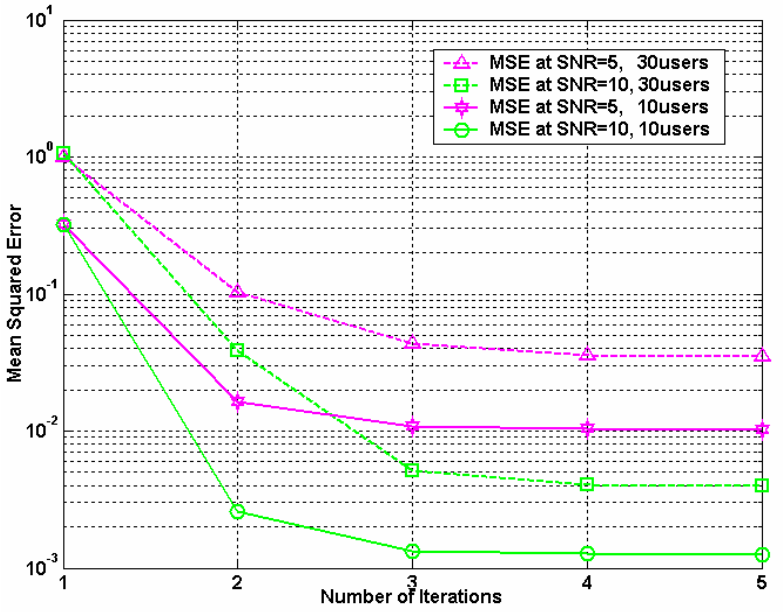

Fig. 3.3. The MSE corresponding to the number of iterations.

The following Fig. 3.4 and Fig. 3.5 are the BER performances of the iterative MUD algorithm with 10 and 30 active users respectively, and the detection

window is also chosen to be three symbols. Since we just sample the strongest path of each coming pulse in our detection process, we choose one-path based MF for a fair performance comparison, both in multiuser and single-user systems.

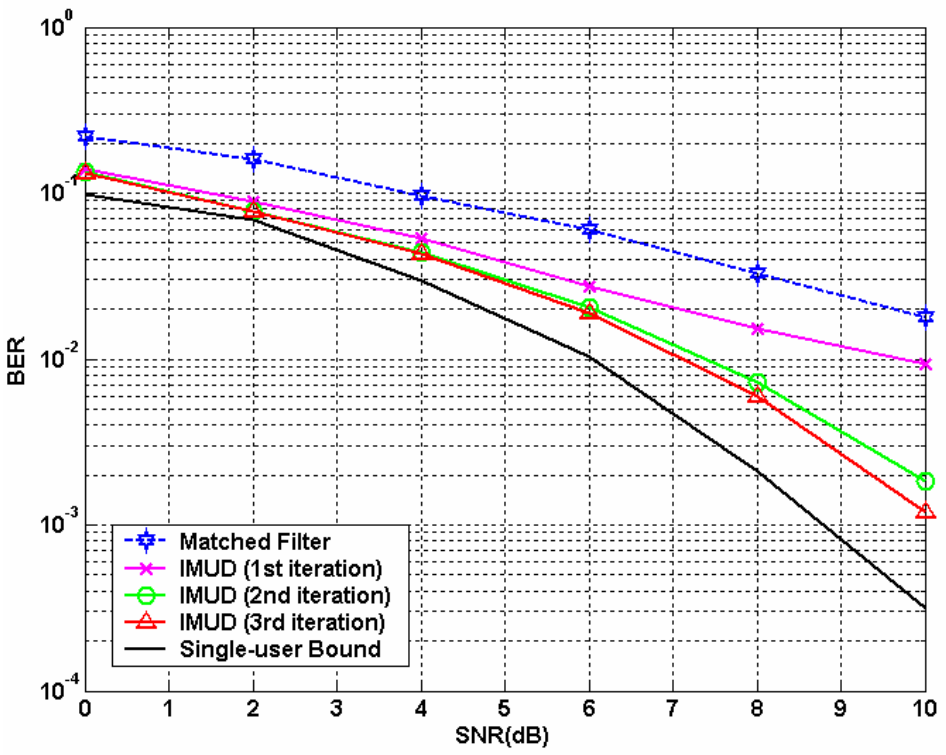

Fig. 3.4. BER performance of the iterative MUD with 10 active users.

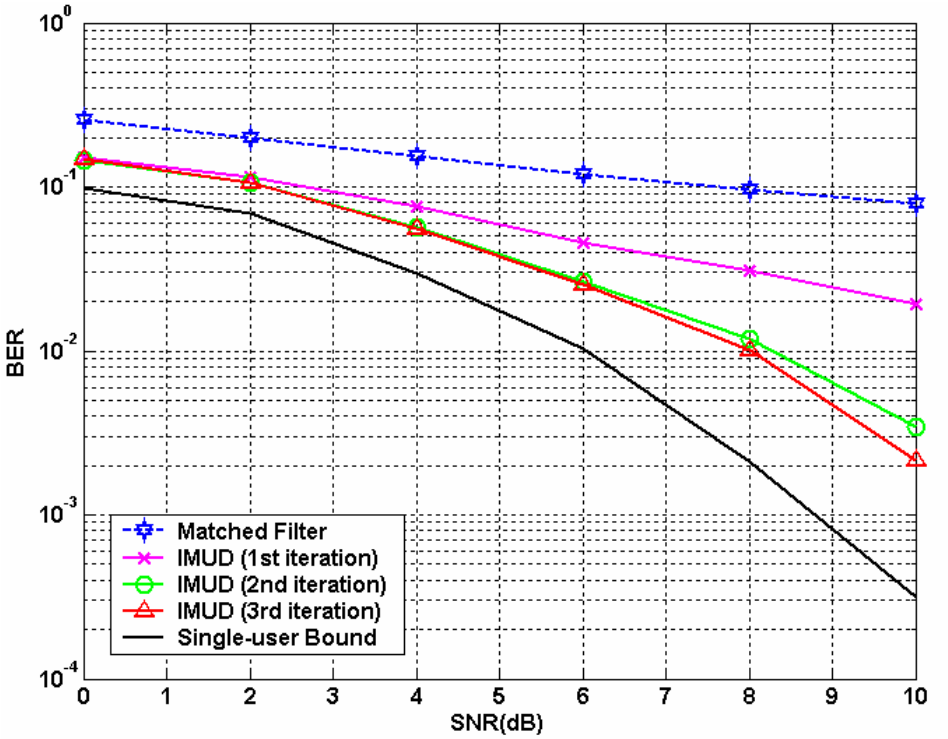

Fig. 3.5. BER performance of the iterative MUD with 30 active users.

Observed from the figures, the simulation results are quite satisfactory in terms of the asynchronous scenario and the low-complexity. And the BER performance of this iterative MUD algorithm would not degrade much with increase in number of users, which is a highly desirable characteristic for multiuser detectors.

We have also studied the characteristics of the detection window. While to our surprise, the simulation results show that the window size may not have an obvious influence on the BER performance, as long as a minimum of three-symbol's duration is chosen. A detection window lasting three symbols is thus used throughout our simulations. We think this result may testify that UWB signaling itself can suppress the inter symbol interference (ISI) and even the inter frame interference (IFI) effectively.

3.4 Summary

In this chapter we propose a low-complexity iterative MUD algorithm specifically designed for TH-UWB systems. The MAP criterion is applied in the detection process by subtracting the MAI precisely. Considering the asynchronous scenario, a truncated detection window is introduced, and the computational complexity for this block decoding is reduced in an iterative manner. The simulation results demonstrate that the proposed iterative MUD algorithm can achieve a satisfactory BER performance while maintaining a considerably low-complexity.

Chapter 4

Low-Complexity Iterative Multiuser Detection for Space-Time Coded UWB Systems

Recently, analog space-time (ST) coding has been introduced into multi-antenna UWB systems and has shown its potential in achieving robust data transmission. In order to exploit the advantages of both multiple-access communications and spatial diversity, we propose in this chapter a low-complexity iterative MUD scheme for analog ST coded multi-antenna UWB systems.

4.1 Introduction

It is generally known that asynchronous transmission is the biggest challenge for MUD issues, where every symbol of each user is possibly interfered by two neighboring symbols from every other user. Thus if we want to figure out the exact MAI suffered by that symbol, it is necessary for us to get the information carried

by those pairs of symbols from every other user, while the detection for which may in turn depend on the information of more symbols either detected or undetected.

In the last chapter we use a suboptimum method, implementing a detection window lasting several symbols long and performing a kind of “block decoding”. Now we want to further reduce the complexity and convert the asynchronous scenario into a somewhat “synchronous” one.

This detection is performed in a two-symbol by two-symbol manner. After the analog ST coding [24], symbols are rearranged and transmitted in pairs. As for the received signal, each pair of symbol information would be mixed and both lasting two symbols long. Since the relative delays across all the users are assumed to be less than one symbol, a one-symbol-long interval can be certainly found out of the two-symbol-long signal section, containing the information of just one pair of symbols from each user and without “symbol overlapping” from the former or later pairs. Fortunately, the information within this interval is enough for our detection due to UWB signal’s abundance in time-spreading. Obviously some of the information (half in the time domain) is ignored, while the ignored part is badly disturbed, and taking the information out of which may cause great trouble and complexity. For the sake of simplicity we implement our detection algorithm within such one-symbol-long intervals. Simulation results show that its performance is actually quite good.

In summary, by using analog ST coding scheme in UWB systems, we can find a way to counteract the problem caused by asynchronous transmission and great simplicity can be achieved.

4.2 System Model

Consider a BPM TH-UWB system with two transmit antennas and one receive antenna, where the analog ST coding scheme proposed in [24] is implemented. That is, in the duration of each two symbols, every frame from these two symbols is alternately transmitted from each of the two transmit antennas. And apparently some of them should be phase-reversed according to the ST coding scheme.

Assume that there are N_u active users in this system. As for the k^{th} user, k taken from 1 to N_u, two consecutive symbols $b_1(k)$ and $b_2(k)$ are alternately transmitted from each of the two transmit antennas 0 and 1 over a duration of two symbols $2N_fT_f$, where T_f and N_f define the frame duration and the number of frames per symbol, respectively.

More specifically, the signal transmitted from antenna 0 is:

$$s_{0,k}(t) = \sum_{j=0}^{N_f-1}\left[b_1(k)\omega\left(t-2jT_f-c(k,j)T_c\right)-b_2(k)\omega\left(t-(2j+1)T_f-c(k,j)T_c\right)\right]. \quad (4.1)$$

And the signal transmitted from antenna 1 is:

$$s_{1,k}(t) = \sum_{j=0}^{N_f-1}\left[b_2(k)\omega\left(t-2jT_f-c(k,j)T_c\right)+b_1(k)\omega\left(t-(2j+1)T_f-c(k,j)T_c\right)\right]. \quad (4.2)$$

Assume that the multipath fading channels are quasi-static over the duration of two symbols. The received noisy waveform is then given by:

$$\begin{aligned} y(t) = \sum_{k=1}^{K}\sum_{j=0}^{N_f-1}\Big[& b_1(k)\lambda_{0,k}\left(t-2jT_f\right)+b_2(k)\lambda_{1,k}\left(t-2jT_f\right) \\ & -b_2(k)\lambda_{0,k}(t-(2j+1)T_f)+b_1(k)\lambda_{1,k}(t-(2j+1)T_f)\Big]+\xi(t) \end{aligned}, \quad (4.3)$$

where $\lambda_{i,k}(t) = \sum_{l=1}^{L} \gamma_{i,k}(l)\omega\left(t - \left(c(k,j)+l\right)T_c - \delta_k\right)$ for i = 0 or 1. And $\xi(t)$ is an AWGN with a spectral density of $N_0/2$ (also with a variance of σ_0^2). Here, $\gamma_{i,k}(l)$ (l=1, …, L) is the gain of the l^{th} multipath related to the k^{th} user and the i^{th} antenna, with a corresponding delay of lT_c after the transmission instance, and δ_k is the relative delay of the k^{th} user. Without loss of generality, we set δ_1=0 and $0 \le \delta_k < T_s$ (k = 2, …, K), where T_s represents the symbol duration.

Similar to the signal model in section 3.1, the definition of multipath here is also based on consecutive chip width labeled 1 to L backwards. We also set L (the maximum number of multipaths under consideration) around N_c (the number of chips per frame), and ignore the others (if there is any). The gain related to a certain pulse width should be set as the summation of the gains of all the arriving paths in that chip duration. Thus, a chip-based discrete-time signal model is also addressed here as that in Chapter 3.

After we get the received waveform $y(t)$, N_u MFs are used to capture the corresponding pulses of the N_u users. The MF related to the k^{th} user samples the received signal only at time instances when the pulses of the k^{th} user arrive via the strongest path, which is assumed to have delay $l_{i,k}T_c$ and gain $\gamma_{i,k}$ (simplified expression for $\gamma_{i,k}(l_{i,k})$) for the i^{th} transmit antenna. It can be easily figured out that these sampling instances are $2jT_f + c(k,j)T_c + \tau_{0,k}$, $2jT_f + c(k,j)T_c + \tau_{1,k}$, $(2j+1)T_f + c(k,j)T_c + \tau_{0,k}$, and $(2j+1)T_f + c(k,j)T_c + \tau_{1,k}$, respectively, for k=1, …, N_u and j=0, …, N_f-1. Here $\tau_{i,k} = \delta_k + l_{i,k}T_c$, and it is assumed that $0 < \tau_{i,k} \le T_s$.

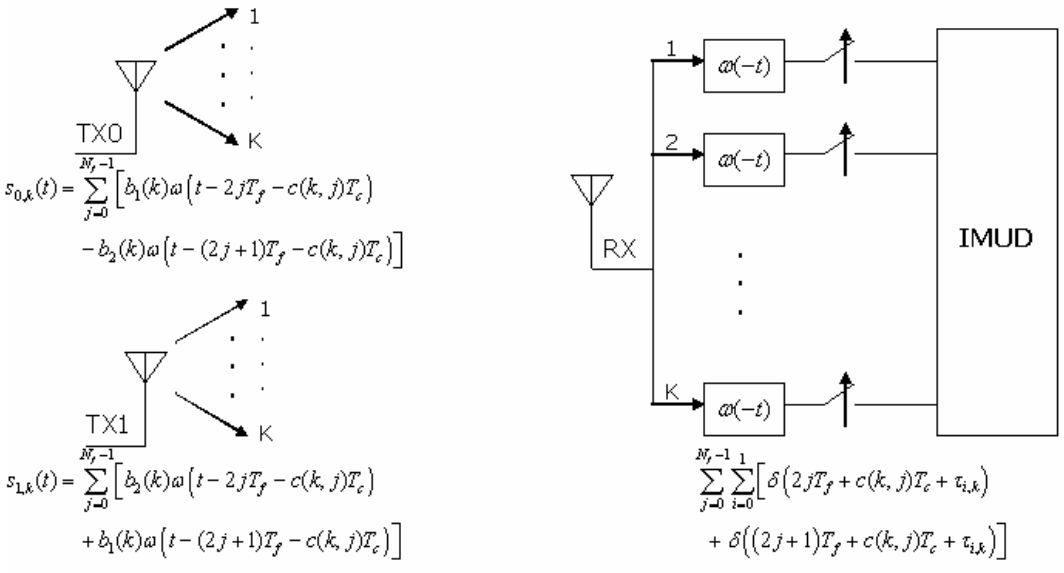

Fig. 4.1. The general structure of the ST-coded UWB system.

According to the chip-based discrete-time signal model, $\tau_{i,k}$ should be multiples of the chip width T_c. If $\tau_{0,k} = \tau_{1,k}$ is met by chance, we just sample once at that time instance. As a result, after the MF we have the chip-sampled discrete-time sequence related to the k^{th} user's even frames:

$$\varphi_k(2j) = b_1(k)\gamma_{0,k} + b_2(k)\gamma_{1,k} + \varsigma_k(2j) + \varepsilon_\omega \sum_{k'=1}^{N_u}\sum_{j'=0,j'\neq j}^{N_f-1} \left[\left(b_1(k')+b_2(k')\right)h_a\left(k',j';k,j\right) + \left(b_1(k')-b_2(k')\right)h_b\left(k',j';k,j\right)\right], \quad (4.4)$$

where $j = 0, \ldots, N_f\text{-}1$. Similarly, related to odd frames we have:

$$\varphi_k(2j+1) = b_1(k)\gamma_{1,k} - b_2(k)\gamma_{0,k} + \varsigma_k(2j+1) + \varepsilon_\omega \sum_{k'=1}^{N_u}\sum_{j'=0,j'\neq j}^{N_f-1} \left[\left(b_1(k')+b_2(k')\right)h_b\left(k',j';k,j\right) + \left(b_1(k')-b_2(k')\right)h_a\left(k',j';k,j\right)\right]. \quad (4.5)$$

Here $\varsigma_k(2j)$ and $\varsigma_k(2j+1)$ are the corresponding noise components, and we define that:

$$h_a(k',j';k,j)=\gamma_{0,k'}\left((2j-2j')N_c+c(k,j)-c(k',j')+{(\delta_k-\delta_{k'})}/{T_c}+{\tau_{0,k}}/{T_c}\right)$$
$$+\gamma_{1,k'}\left((2j-2j')N_c+c(k,j)-c(k',j')+{(\delta_k-\delta_{k'})}/{T_c}+{\tau_{1,k}}/{T_c}\right), \quad (4.6)$$

and

$$h_b(k',j';k,j)=\gamma_{0,k'}\left((2j-2j'-1)N_c+c(k,j)-c(k',j')+{(\delta_k-\delta_{k'})}/{T_c}+{\tau_{0,k}}/{T_c}\right)$$
$$+\gamma_{1,k'}\left((2j-2j'-1)N_c+c(k,j)-c(k',j')+{(\delta_k-\delta_{k'})}/{T_c}+{\tau_{1,k}}/{T_c}\right). \quad (4.7)$$

As can be seen from (4.4) and (4.5), we've considered possible pulse collisions due to multipath effects within the same symbol across all the users. The equations here may look quite complicated, while actually they are straightforward, and similar to the analysis of channel impact in Chapter 3. The actual MAI should be much less than what we have specified here, basically one pulse being affected by one or two neighboring pulses from every other user, but we just write everything down in order to be rigorous.

Since both $\varphi_k(2j)$ and $\varphi_k(2j+1)$ contain the information of these two symbols, a scheme similar to the MRC is used to combine them, and the resultant $r_{k,1}(j)$ and $r_{k,2}(j)$, which mainly represent the information of symbol 1 and symbol 2, respectively, are fed to the iterative MUD. Notice that $\gamma_{i,k}$ stands for the pulse-sampled value of the strongest path of the pulses related to the k^{th} user and the i^{th} transmit antenna.

$$r_{k,1}(j) = \gamma_{0,k}\varphi_k(2j) + \gamma_{1,k}\varphi_k(2j+1)$$

$$= \left(\gamma_{0,k}^2 + \gamma_{1,k}^2\right) b_1(k) + \underbrace{\gamma_{0,k}\varsigma_k(2j) + \gamma_{1,k}\varsigma_k(2j+1)}_{\eta_{k,1}(j)} + \varepsilon_m \sum_{k'=1}^{N_u} \sum_{j'=0, j'\neq j}^{N_f-1} \tag{4.8}$$

$$\left[\left(b_1(k') + b_2(k')\right) H_0(k', j'; k, j) + \left(b_1(k') - b_2(k')\right) H_1(k', j'; k, j)\right]$$

In the equation above, $H_0(k', j'; k, j) = \gamma_{0,k} h_a\left(k', j'; k, j\right) + \gamma_{1,k} h_b\left(k', j'; k, j\right)$ and $H_1(k', j'; k, j) = \gamma_{0,k} h_b\left(k', j'; k, j\right) - \gamma_{1,k} h_b\left(k', j'; k, j\right)$ are assumed to make it more concise. Similarly we can deduce:

$$r_{k,2}(j) = \gamma_{1,k}\varphi_k(2j) - \gamma_{0,k}\varphi_k(2j+1)$$

$$= \left(\gamma_{0,k}^2 + \gamma_{1,k}^2\right) b_2(k) + \underbrace{\gamma_{1,k}\varsigma_k(2j) - \gamma_{0,k}\varsigma_k(2j+1)}_{\eta_{k,2}(j)} + \varepsilon_m \sum_{k'=1}^{N_u} \sum_{j'=0, j'\neq j}^{N_f-1} . \tag{4.9}$$

$$\left[\left(b_1(k') - b_2(k')\right) H_0(k', j'; k, j) - \left(b_1(k') + b_2(k')\right) H_1(k', j'; k, j)\right]$$

Similar to Chapter 3, the noise components $\eta_{k,1}(j)$ and $\eta_{k,2}(j)$ can still be assumed to be white, and their variances can be calculated as:

$$\sigma_{\eta_{k,1}}{}^2 = \left(\gamma_{0,k}^2 + \gamma_{1,k}^2\right)\varepsilon_m \sigma_0{}^2 = \sigma_{\eta_{k,2}}{}^2 . \tag{4.10}$$

4.3 Iterative Multiuser Detection

This iterative MUD algorithm is based on the *r*'s we've already got. As specified before, the sequence we actually use is not the whole but within an interval of one symbol's duration, where two consecutive pairs of symbols from a single user do not coexist. Without loss of generality, these *r*'s used for detection can be sorted as 1 to $\lfloor N_f/2 \rfloor$ in this interval for each user.

Let $\Phi_{k,g}$ represents the likelihood ratio of the MAP probabilities for $b_g(k)$ equaling to either 1 or -1. The following shows how to deduce $\Phi_{k,g}(n+1)$ from $\Phi_{k,g}(n)$, where n indexes the cycle of iterations.

Define

$$\Phi_{k,g}(n+1) = \ln \frac{\Pr\left(b_g(k)=1 \mid r_{k,g}(1), r_{k,g}(2), ..., r_{k,g}\left(\left\lfloor N_f/2 \right\rfloor\right)\right)}{\Pr\left(b_g(k)=-1 \mid r_{k,g}(1), r_{k,g}(2), ..., r_{k,g}\left(\left\lfloor N_f/2 \right\rfloor\right)\right)}, \tag{4.11}$$

for g=0 or 1. Similar to Chapter 3, we treat all the $r_{k,g}$'s as independent random variables, and based on the Bayes' rule we can further get:

$$\Phi_{k,g}(n+1) = \left\lfloor N_f/2 \right\rfloor \Phi_{k,g}(n) + \sum_{j=1}^{\lfloor N_f/2 \rfloor} \ln \frac{f\left(r_{k,g}(j) \mid b_g(k)=1\right)}{f\left(r_{k,g}(j) \mid b_g(k)=-1\right)}. \tag{4.12}$$

Since $\Phi_{k',g}(n)$, k' taken from 1 to N_u, has already been obtained in the last iteration, from its definition we can easily deduce a soft estimation of $b_g(k')$:

$$E\left\{b_g(k')\right\} = \tanh\left(\tfrac{1}{2}\Phi_{k',g}(n)\right). \tag{4.13}$$

The substitution of (4.8) into (4.12) yields:

$$\Phi_{k,1}(n+1) = \left\lfloor N_f/2 \right\rfloor \Phi_{k,1}(n) + \sum_{j=1}^{\lfloor N_f/2 \rfloor} \ln \frac{f\left(\begin{array}{l} \gamma_{0,k}^2 + \gamma_{1,k}^2 + \eta_{k,1}(j) + \varepsilon_m \sum_{k'=1}^{N_u} \sum_{j'=0, j'\neq j}^{N_f-1} \\ \left[\left(b_1(k')+b_2(k')\right)H_0(k',j';k,j) + \left(b_1(k')-b_2(k')\right)H_1(k',j';k,j)\right] \end{array}\right)}{f\left(\begin{array}{l} -\gamma_{0,k}^2 - \gamma_{1,k}^2 + \eta_{k,1}(j) + \varepsilon_m \sum_{k'=1}^{N_u} \sum_{j'=0, j'\neq j}^{N_f-1} \\ \left[\left(b_1(k')+b_2(k')\right)H_0(k',j';k,j) + \left(b_1(k')-b_2(k')\right)H_1(k',j';k,j)\right] \end{array}\right)}. \tag{4.14}$$

Similarly, the substitution of (4.9) into (4.12) yields:

$$\Phi_{k,2}(n+1)=\lfloor N_f/2\rfloor\Phi_{k,2}(n)+$$
$$\sum_{j=1}^{\lfloor N_f/2\rfloor}\ln\frac{f\left(\begin{array}{l}\gamma_{0,k}^2+\gamma_{1,k}^2+\eta_{k,2}(j)+\varepsilon_m\sum_{k'=1}^{N_u}\sum_{j'=0,j'\neq j}^{N_f-1}\\ \left[\left(b_1(k')-b_2(k')\right)H_0(k',j';k,j)-\left(b_1(k')+b_2(k')\right)H_1(k',j';k,j)\right]\end{array}\right)}{f\left(\begin{array}{l}-\gamma_{0,k}^2-\gamma_{1,k}^2+\eta_{k,2}(j)+\varepsilon_m\sum_{k'=1}^{N_u}\sum_{j'=0,j'\neq j}^{N_f-1}\\ \left[\left(b_1(k')-b_2(k')\right)H_0(k',j';k,j)-\left(b_1(k')+b_2(k')\right)H_1(k',j';k,j)\right]\end{array}\right)}.$$
(4.15)

Based on the Central Limit Theorem, it can be well assumed that the part of MAI in (4.14) is Gaussian, with mean and variance as follows:

$$\mu_{I_{k,1}}=\sum_{k'=1}^{N_u}\sum_{j'=0,j'\neq j}^{N_f-1}\left[\begin{array}{l}\left(H_0(k',j';k,j)+H_1(k',j';k,j)\right)\tanh\left(\frac{1}{2}\Phi_{k',1}(n)\right)\\ +\left(H_0(k',j';k,j)-H_1(k',j';k,j)\right)\tanh\left(\frac{1}{2}\Phi_{k',2}(n)\right)\end{array}\right],\qquad(4.16)$$

$$\sigma_{I_{k,1}}^2(n)=\sum_{k'=1}^{N_u}\sum_{j'=0,j'\neq j}^{N_f-1}\left[\begin{array}{l}\left(H_0(k',j';k,j)+H_1(k',j';k,j)\right)^2\left(1-\tanh^2\left(\frac{1}{2}\Phi_{k',1}(n)\right)\right)\\ +\left(H_0(k',j';k,j)-H_1(k',j';k,j)\right)^2\left(1-\tanh^2\left(\frac{1}{2}\Phi_{k',2}(n)\right)\right)\end{array}\right].$$
(4.17)

Similarly, we can derive the mean and variance for the MAI in (4.15) as:

$$\mu_{I_{k,2}}=\sum_{k'=1}^{N_u}\sum_{j'=0,j'\neq j}^{N_f-1}\left[\begin{array}{l}\left(H_0(k',j';k,j)-H_1(k',j';k,j)\right)\tanh\left(\frac{1}{2}\Phi_{k',1}(n)\right)\\ -\left(H_0(k',j';k,j)+H_1(k',j';k,j)\right)\tanh\left(\frac{1}{2}\Phi_{k',2}(n)\right)\end{array}\right],\qquad(4.18)$$

$$\sigma_{I_{k,2}}^2(n)=\sum_{k'=1}^{N_u}\sum_{j'=0,j'\neq j}^{N_f-1}\left[\begin{array}{l}\left(H_0(k',j';k,j)-H_1(k',j';k,j)\right)^2\left(1-\tanh^2\left(\frac{1}{2}\Phi_{k',1}(n)\right)\right)\\ +\left(H_0(k',j';k,j)+H_1(k',j';k,j)\right)^2\left(1-\tanh^2\left(\frac{1}{2}\Phi_{k',2}(n)\right)\right)\end{array}\right].$$
(4.19)

In accordance with (4.10) and (4.16)-(4.19), (4.12) can be further expressed as follows:

$$\Phi_{k,g}(n+1) = \lfloor N_f/2 \rfloor \Phi_{k,g}(n) + \sum_{j=1}^{\lfloor N_f/2 \rfloor} \left[\frac{2\left(\gamma_{0,k}^2 + \gamma_{1,k}^2\right)\left(r_{k,g}(j) - \mu_{I_{k,g}}\right)}{\sigma_{I_{k,g}}^2(n) + \sigma_{\eta_{k,g}}{}^2} \right]. \quad (4.20)$$

Notice that this joint detection produces $2N_u$ symbols at the same time over each duration of two consecutive symbols $2N_fT_f$. And the computational complexity for each time of iteration is $O(N_u^2)$.

4.4 Simulation Results and Discussions

In the computer based simulations, we consider a BPAM TH-UWB system with two transmit antennas and one receiver antenna. The channels are generated according to Foerster's database of impulse radio channels [10], CM1 also. The chip (pulse) duration T_c=1ns, chip number N_c =50, frame number N_f=10, thus each user transmits at a data rate of 2 Mbps.

Fig. 4.2 to Fig. 4.4 are the BER performances of the iterative MUD algorithm with respectively 10, 20 and 30 active users. The results are quite satisfactory in terms of the asynchronous scenario and the low-complexity. The performance of the proposed iterative MUD in the case of single-antenna UWB system (without ST-coding) is also plotted. Obviously, a BER performance improvement of around 3dB can be achieved.

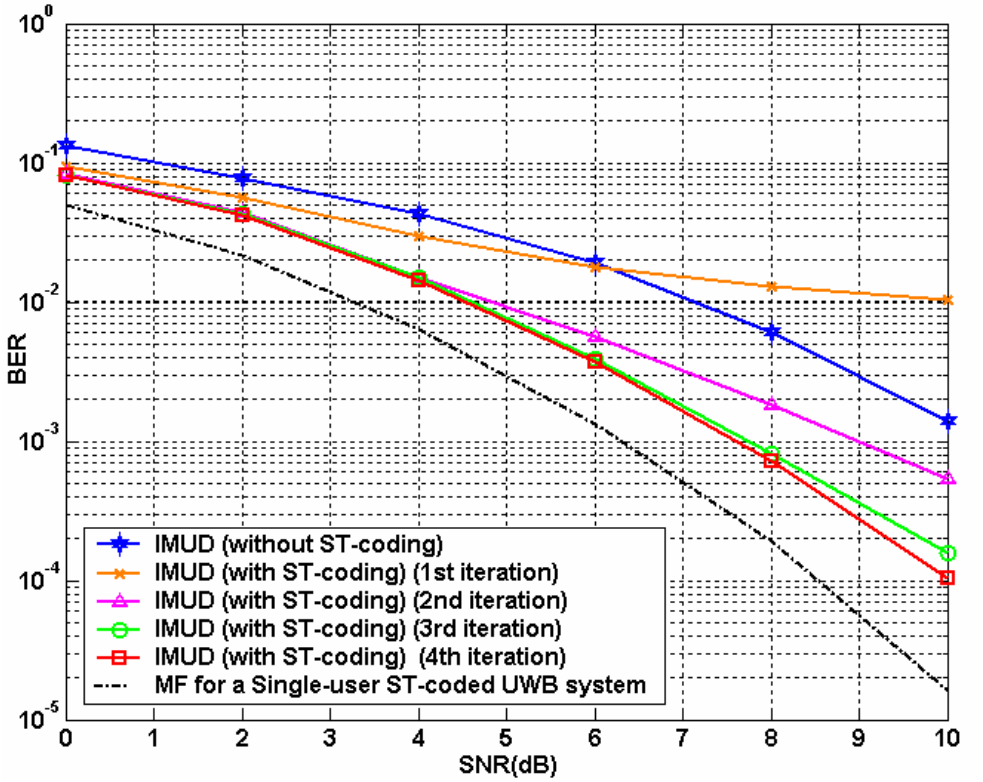

Fig. 4.2. BER comparison for a 10-user ST coded UWB system.

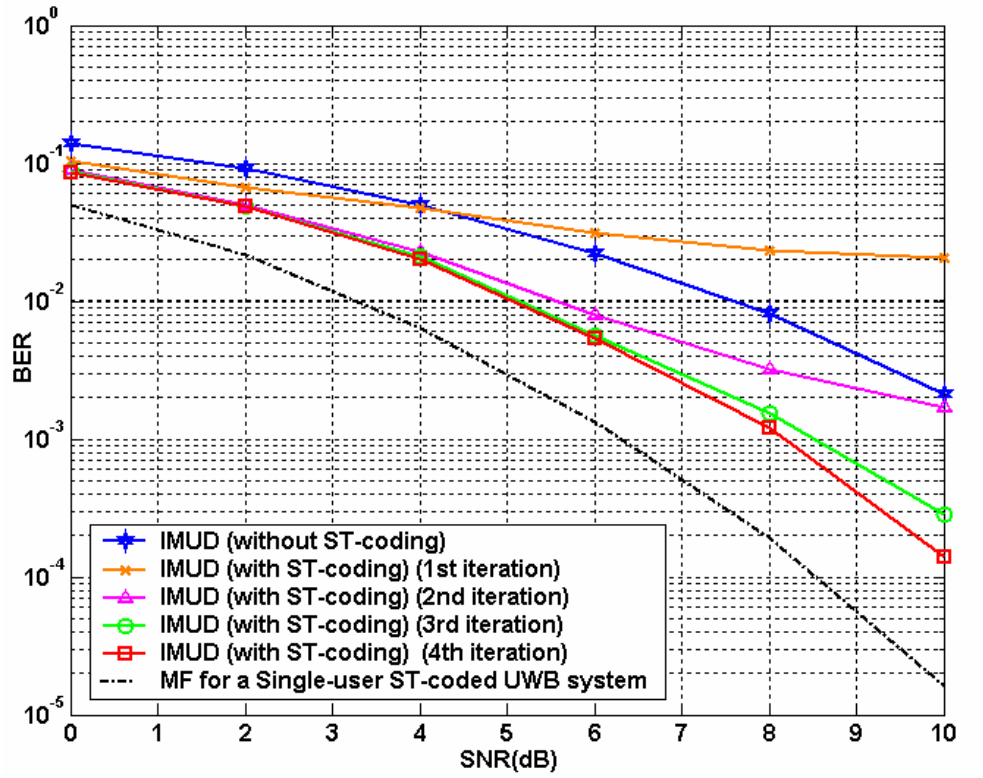

Fig. 4.3. BER comparison for a 20-user ST coded UWB system.

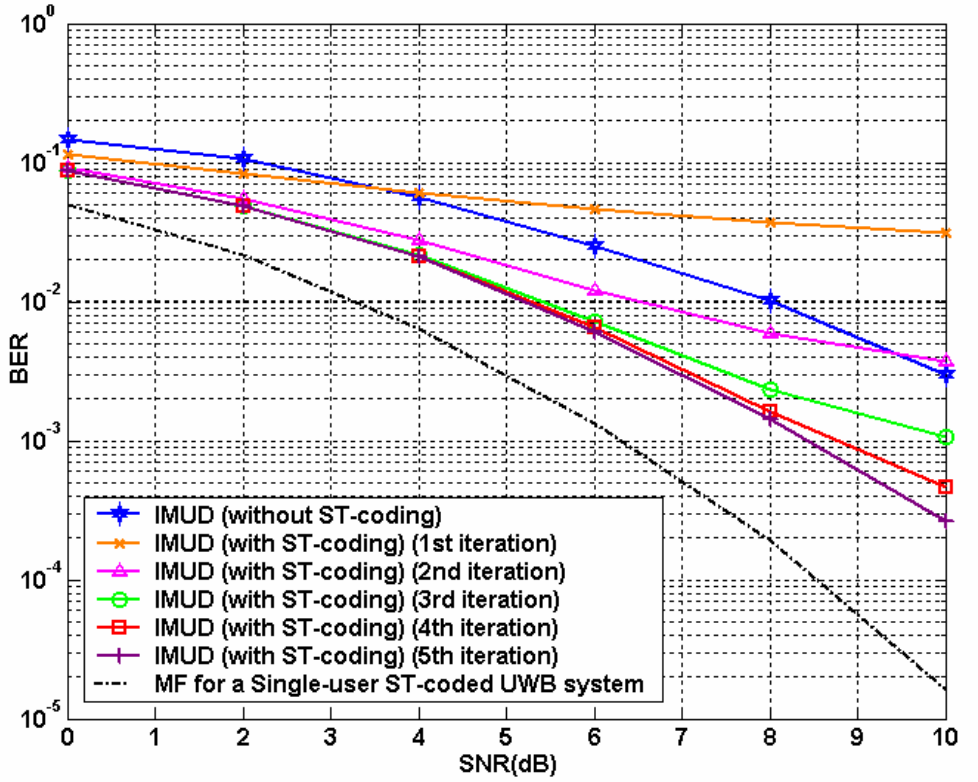

Fig. 4.4. BER comparison for a 30-user ST coded UWB system.

4.5 Summary

We have extended the already proposed iterative MUD algorithm to ST coded multi-antenna UWB systems in this chapter. We aim to combine the advantages of both UWB technology and ST coding. After using an analog ST coding scheme, we also find a way to further reduce the complexity. Computer based simulations have demonstrated its satisfactory BER performance and low complexity.

Chapter 5

Conclusions and Future Work

5.1 Conclusions

Impulse radio is a technique with a long history going back to the 1960's, and has recently been revitalized in indoor wireless applications. The rising popularity of this technique, commonly referred to as UWB technology, mainly comes from the recently released spectrum bandwidth specified for it, as well as its promising features over normal narrowband communication systems, such as low power, low cost, high data rate and well stability.

As for the MUD for multiple access UWB systems, most of the popular receivers seem to be simple applications of standard MUD methods to UWB systems, which may not be quite satisfactory in terms of both the computational complexity and the BER performance.

In this thesis, a novel iterative MUD algorithm specifically designed for UWB systems is proposed, which features low-complexity and good BER performance. This algorithm is based on the MAP criterion by iteratively

subtracting the MAI. Moreover, a truncated detection window is used in face of the asynchronous transmission of multiple users. Simulation results have demonstrated our theoretical analysis.

Another contribution is the even lower complexity extension of this algorithm to ST coded multi-antenna UWB systems. By using the analog ST coding scheme, we can further deduce the complexity and improve the system performance. Also, the detection problem caused by asynchronous transmission can be intentionally avoided.

5.2 Future Work

The proposed low-complexity iterative MUD algorithm seems to be the first effort made to implement iterative MUD algorithms to asynchronous UWB systems, as well as ST-coded multi-antenna UWB systems. Further examinations can be carried out to evaluate the performance of this algorithm, for instance its capability under various interferences, or the study of the BER performance vs. number of multiple users.

In this algorithm we just sampled the strongest path of each transmitted pulse as the desired information, which can be called as one-path based iterative MUD. Obviously things should be better if we can combine several paths' information. This work may relay on favorable and novel combination schemes, either prior, in between, or posterior to the detection process, otherwise the complexity will increase remarkably.

It is also recommended to develop new and related iterative MUD algorithms for other coding schemes, for example Turbo coding.

Noticeably, this proposed algorithm requires perfect channel information, and synchronization to the desired symbols. Thus the problem of channel estimation and synchronization become especially important. Actually we think these two problems are quite essential in all the detection issues related to UWB, which is really sensitive to channel estimation and timing errors. The investigation of these two problems could be tough while significant.

References

[1] "Wireless networking overview," http://www.microsoft.com/resources/documentation/windows/xp/all/proddocs/en-us/wireless_networking_overview.mspx.

[2] "Ultra-wideband (UWB) technology," http://www.intel.com/technology/ultrawideband/downloads/Ultra-Wideband.pdf.

[3] T. S. Rappaport, *Wireless Communications: Principles and Practice*, Upper Saddle River, NJ, Printice Hall, 1996.

[4] J. Foerster, E. Green, S. Somayazulu, and D. Leeper, "Ultra-wideband technology for short- or medium-range wireless communications," *Intel Technology Journal*, Q2, 2001.

[5] L. E. Miller, "Why UWB? a review of ultra-wideband technology," http://www.antd.nist.gov/wctg/manet/NIST_UWB_Report_April03.pdf.

[6] M. O. Wessman and A. Svensson, "Comparison between DS-UWB, multiband UWB and multiband OFDM on IEEE UWB channels," *Proc. Nordic Radio Symposium and Finnish Wireless Communications Workshop*, Oulu, Finland, Aug 2004.

[7] R. A. Scholz, “Multiple access with time-hopping impulse modulation,” *IEEE Conf. MILCOM*, Oct. 11-14, 1993.

[8] M. Z. Win and R. A. Scholtz, “Impulse radio: how it works,” *IEEE Communications Letters*, vol. 2, no. 2, pp. 10-12, Jan. 1998.

[9] I. Guvenc and H. Arslan, "On the modulation options for UWB systems", *IEEE Conf. MILCOM*, Boston, USA, Oct. 2003.

[10] J. Foerster, “Channel modeling sub-committee report final,” *IEEE* P802.15 02/490rl-SG3a, Feb. 2003.

[11] D. Cassioli, M. Z. Win, F. Vatalaro, and A. F. Molisch, “Performance of low-complexity Rake reception in a realistic UWB channel,” *IEEE Conf. ICC2002*, Vol. 2, 28 April-2 May, 2002.

[12] A. Rajeswaran, V. S. Somayazulu, and J. Foerster, “Rake performance for a pulse based UWB system in a realistic UWB indoor channel,” *IEEE Conf. ICC 2003*, vol. 4, 11-15 May, 2003.

[13] Q. Li and L. A. Rusch, “Hybrid RAKE / multiuser receivers for UWB,” *IEEE Conf. RAWCON 2003*, 10-13 Auguest, 2003.

[14] Y. C. Yoon and R. Kohno, “Optimum multi-user detection in ultra-wideband (UWB) multiple-access communication systems,” *IEEE Conf. ICC 2002*, Vol. 2, April, 2002.

[15] S. Verdu, *Multiuser Detection*, Cambridge University Press, 1998.

[16] N. Boubaker and K. B. Letaief, “A low complexity MMSE-RAKE receiver in a realistic UWB channel and in the presence of NBI,” *IEEE Conf. WCNC 2003*, vol. 1 , 16-20 March 2003.

[17] A. Bayesteh, and M. Nasiri-Kenari, , "Iterative interference cancellation and decoding for a coded UWB-TH-CDMA system in multipath channels using MMSE filters," *IEEE Conf. PIMRC 2003*, vol. 2, pp. 1555-1559, 7-10 Sept. 2003.

[18] M. J. Juntti, B. Aazhang, and J. O. Lilleberg, "Iterative implementation of linear multiuser detection for dynamic asynchronous CDMA systems," *IEEE Trans. Commun.,* Vol. 46, Issue 4, pp: 503 -508, April 1998.

[19] M. Moher and P. Guinand, "An iterative algorithm for asynchronous coded multiuser detection," *IEEE Communications Letters*, Vol. 2, pp: 229 -231, Aug. 1998.

[20] K. Yen and L. Hanzo, "Genetic algorithm assisted multiuser detection in asynchronous CDMA communications," *IEEE Conf. ICC 2001*, Vol. 3, pp: 826 -830, June 2001.

[21] M. J. Juntti, B. Aazhang, and J. O. Lilleberg, "Iterative implementation of linear multiuser detection for dynamic asynchronous CDMA systems," *IEEE Trans. Commun*., Vol. 46 pp: 503 -508, April 1998.

[22] E. Fishler and H. V. Poor, "Iterative ("turbo") multiuser detectors for impulse radio systems," submitted to *IEEE Trans. Commun.*.

[23] E. Fishler and H. V. Poor, "Low-complexity multi-user detectors for time hopping impulse radio systems," submitted to *IEEE Trans. Signal Processing*.

[24] L. Yang and G. B. Giannakis, "Analog space-time coding for multi-antenna ultra-wideband transmissions," *IEEE Trans. Commun.*, vol. 52, pp. 507-517, March 2004.

[25] Q. Li and L. A. Rusch, , "Multiuser detection for DS-CDMA UWB in the home environment," *IEEE J. Select. Areas Commun.*, vol. 20, pp. 1701-1711, Dec. 2002.

[26] M. Z. Win and R. A. Scholtz, "Ultra-wide bandwidth time-hopping spread-spectrum impulse radio for wireless multiple-access communications," *IEEE Trans. Commun.*, vol. 48, pp. 679-691, April 2000.

[27] J. G. Proakis, *Digital Communications*, 4th edition, McGraw-Hill, 1983.

Published Papers by the Author

[1] XiaoLi Wang, Lei Huang and ChiChung Ko, "Iterative multiuser detection for space-time coded ultra-wideband systems," *IEEE Conf. ICCCAS04*, vol. 1, pp. 89-92, June, 2004.

[2] XiaoLi Wang, Lei Huang and ChiChung Ko, "Low-complexity iterative MUD for asynchronous UWB systems," *IEEE Conf. ICCS2004*, Sept., 2004.